Technical Report

TR-98-11

# Leaching of 90-year old concrete mortar in contact with stagnant water

Jan Trägårdh and Björn Lagerblad

Swedish Cement and Concrete Research Institute

July 1998

**Svensk Kärnbränslehantering AB**
Swedish Nuclear Fuel
and Waste Management Co
Box 5864
SE-102 40 Stockholm Sweden
Tel 08-459 84 00
+46 8 459 84 00
Fax 08-661 57 19
+46 8 661 57 19

# Leaching of 90-year old concrete mortar in contact with stagnant water

Jan Trägårdh and Björn Lagerblad

Swedish Cement and Concrete Research Institute

July 1998

This report concerns a study which was conducted for SKB. The conclusions and viewpoints presented in the report are those of the author(s) and do not necessarily coincide with those of the client.

Information on SKB technical reports from1977-1978 (TR 121), 1979 (TR 79-28), 1980 (TR 80-26), 1981 (TR 81-17), 1982 (TR 82-28), 1983 (TR 83-77), 1984 (TR 85-01), 1985 (TR 85-20), 1986 (TR 86-31), 1987 (TR 87-33), 1988 (TR 88-32), 1989 (TR 89-40), 1990 (TR 90-46), 1991 (TR 91-64), 1992 (TR 92-46), 1993 (TR 93-34), 1994 (TR 94-33), 1995 (TR 95-37) and 1996 (TR 96-25) is available through SKB.

## Abstract (English)

Concrete and other cementitious materials will be used for different purposes in the underground repositories for radioactive waste in the form of spent fuel according to the Swedish concept. Cementitious materials are fundamentally unstable in water and will change properties with time. Thus it is important to know the long-term interaction between the cement-based materials, groundwater and the other materials in the repository that are important for the safety. This report concerns a study of diffusion controlled dissolution of mortar in a case study.

In 1906 a water tank was installed in one of the towers in the castle of Uppsala, Sweden. A 20 mm thick layer of concrete mortar was placed on the inner walls of a steel canister which compriced the water tank. It was demolished in 1991 and pieces of the mortar were taken for analysis. The water tank has been refilled periodically with fresh water, which means that the mortar has been leached by drinking water for nearly 85 years. As the steel hinders the penetration of water, diffusion processes must have controlled the leaching.

The concrete has been investigated by several methods including thin sections in a polarising microscope, SEM, SEM-EDS, image analysis and chemical analysis. The result shows that the mortar is covered by a thin shell of carbonates presumably reaction products between the cementpaste and bicarbonates from the water. Behind the carbonated surface to a depth of around 5-8 mm the mortar shows a distinct porous zone decreasing calcium contents. At the same time there is a relative increase in the sulphate, aluminium and iron concentrations. This indicates that the leaching is fairly complicated and linked to a recrystallisation and redistribution of element. Behind this depth the paste is dense and has a fairly normal composition except for a slight calcium depletion

The SEM analysis shows that there is no distinct portlandite (calciumhydroxide crystals) depletion front. Portlandite is less frequent in the outer zone but it can be found straight through the uncarbonated mortar. During leaching, the portlandite has recrystallised to coarser aggregates and the calciumsilicatehydrates have reorganised to a lower Ca/Si ratio.

In conclusion, the mortar from the water tank shows that diffusion controlled leaching is more complicated and less effective than previously assumed. Data from leaching tests do not consider long-time structural changes and remobilization of the paste structure. This must be considered in calculation models.

## Abstract (Swedish)

I den Svenska modellen för långtidsförvaring av radioaktivt avfall från använt kärnbränsle kommer betong och andra cementbaserade material att användas för olika ändamål. Förvaringen är tänkt att ske i djupt liggande bergrum vilket medför att dessa material kommer att användas inom olika användningsområden, till exempel för sprickinjektering. I kontakt med vatten är cementbaserade material i grunden kemiskt instabila sett i ett långtidsperspektiv. De cementbaserade materialens struktur kommer därmed sakta att förändras och omfattningen av omvandlingen bestämms till stor del av sammansättningen på det omgivande vattnet och cementet och av tranportmekanismer. Det är därför viktigt att nå kunskap om både grundvattnets och de cementbaserade materialens långtidsförändringar i ett tänkt djupförvar. Denna rapport redovisar en fältstudie av diffussionsstyrd lakning av en gammal cementpasta i kontakt med dricksvatten.

1906 blev en vattentank installerad i ett torn i Uppsala slott. På insidan av en stålbehållare murades ett cirka 20 mm tjockt lager av betongbruk som omslöt dricksvattnet. Vattentanken revs 1991 och bitar av betongbruket blev tillvaratagna för analys av Cement och Betong Institutet (CBI) på uppdrag av Svensk Kärnbränslehantering AB (SKB). Påfyllning av färskt dricksvatten har skett med jämna intervall, vilket betyder att betongbruket har varit påverkat av urlakningsmekanismer i nästan 85 år. Den täta stålväggen på betongbrukets insida har medfört att jonvandringen huvudsakligen har skett från betongbrukets porlösningar till det omgivande dricksvattnet för att utjämna den kemiska potentialskillnaden, dvs. diffussionsstyrd lakning.

Undersökningen av betongbrukets kemi, mineralogi och struktur omfattar flera olika metoder som ljusmikroskopi, SEM, SEM-EDS, bildbehandling och kemisk analys. Resultaten visar att betongbrukets yttersta millimeter består av karbonater som troligen är en produkt av reaktioner mellan lösta bikarbonater i dricksvattnet och cementpastan s.k karbonatisering. Innanför den karbonatiserade zonen och till ett djup av 5-8 mm förekom en tydlig zon med högre porositet och lägre kalciumhalt. I samma zon förekom relativt höga koncentrationer av sulfat, aluminium och järn. Detta visar att lakningsprocessen följer ett ganska komplicerat förlopp som innefattar omfördelning av element genom lösning, utfällning och omkristallisering av mineral. På större djup är cementpastan tätare och har en ganska normal sammansättning med undantag för något lägre kalciumhalter.

Portlanditkristaller förekom mindre frekvent i den porösa zonen men finns i hela cementpastant. Jonvandring i cementpastan har medfört en omfördelning av kalcium och

omkristallisering av portlandit i grövre kristaller samtidigt som Ca/Si-förhållandet i kalciumsilikathydraterna minskade.

Resultaten från undersökningen av betongbruket i vattentanken visar att diffussionsstyrd lakning av cementpasta är mer komplicerad och mindre effektiv än vad man tidigare trott. Tidigare laboratorieförsök med lakningstester har oftast inte tagit hänsyn till cementpastans mognadsgrad, omkristallisering och omstrukturering. Detta måste man ta hänsyn till i framtida beräkningsmodeller.

## Table of contents


**1 Orientation** 1

**2 Introduction** 1

**3 Methods** 3

3.1 Element distribution 3

3.2 Structural features and distribution of mineral phases 4

3.2.1 Electron microscopy (SEM) 4

3.2.2 Thin section study 4

3.3 Porosity 4

**4 Results** 5

4.1 Element distribution 5

4.2 Structural features and distribution of mineral phases 8

4.3 Porosity 9

**5 Summary of results** 10

**6 Discussion** 12

**7 References** 14


## Appendixes


Appendix 1: Structural features (SEM)

Appendix 2: Structural features (Thin section)

Appendix 3: Porosity

Appendix 4: Element distribution

# 1 Orientation

Nuclear waste must be stored for a very long time in such a way that it does not harm the present or future generations of human beings. In Sweden, the waste will be stored in underground repositories that, with time, will be below groundwater level.

In the repositories, cement-based materials will be used in several applications. Thus it is important to know the long-term interaction between the cement-based materials, groundwater and the other materials in the repository that are important for safety. A conceptual model for concrete long-term degradation in a deep nuclear waste repository is published in SKB TR 95-31. This is complemented by some case studies in SKB AR 96-01

Cement-based materials are fundamentally unstable in a long-term perspective. The cement paste contains porefluids with a very high pH and the cement hydration phases are stabilised by this high pH. Thus, with time, the pore fluids will equilibrate with the ground water. This will give a high pH-plume and destabilise the cementpaste. Moreover, the cementpaste was formed during a very short time by coupled dissolution precipitation processes. Thus the cementpaste is not in equilibrium and one can expect reorganisation and recrystallization to a lower energy state with time.

Leaching behaviour has mainly been deduced from experiments. The time periods for the leaching experiments is, however, short and may thus give wrong results as regard long-term performance. This was indicated by an old mortar that has been used as an inside protection in an old water tank from 1906 (SKB AR 96-01). The leaching was much less than expected. This report investigates this water tank in much greater detail.

# 2 Introduction

In 1906 a water tower from the 18th century serving the castle in the town of Uppsala with drinking water, was modernised. A 20-mm thick layer of concrete mortar was placed on the inner walls of a steel canister making up the water tank. The water tank was demolished in 1991 and samples from the concrete mortar were delivered to CBI from Bjerkings Ingenjörsbyrå AB in Uppsala.

The water tank has been refilled periodically with fresh water, which means that equilibrium conditions between the water in the tank and the pore water in the mortar never have been established. The transportation of soluble components in the mortar has been diffusion-

controlled as no water could pass trough it. The concrete mortar has been water saturated and in contact with stagnant water for a period of 85 years. We do not, however, have control over where the individual pieces of mortars come from. The low depth of carbonation indicates that all the sampled pieces of mortar have been submerged in water for most of the time.

The current study includes the determination of the element distribution and the porosity along two cross sections in the concrete mortar of two samples, as well as identification of some structural features. An estimation of the abundance of calcium carbonate and calcium hydroxide phases along a cross section and determination of the bulk calcium content in the cement paste, was also carried out.

# 3 Methods

## 3.1 Element distribution

Determination of the major element distribution along two different cross sections of the concrete mortar was carried out by SEM-EDS equipment. The thickness of the concrete mortar was about 13 mm in sample 1 and 18 mm in sample 2. The elements Ca, Si, Al, S, Mg, K, Na, Fe, Ti, Mn, P and Cl were analysed along traverses shown in Appendix 1 page 1. Each traverse contained at least five analyses and mean values and standard deviations were calculated from each traverse. In this way, element profiles were established through the concrete mortar. The results from element profiles of the two different samples in the watertank, including the elements Ca, Si, Al, S, Mg, K, Na and Fe, are shown in Appendix 4. The elements are presented in the form of wt % oxide, normalised to 100 %.

The analysed fields were about 5 microns or less in order to avoid interference from aggregates in the analysis.

The instrument was calibrated against reference materials, a cement mortar sample with known composition and a pure wollastonite. The detection limits (wt %) for some elements are as follows: Ca (0.09), Si (0.08), Al (0.07), Mg (0.1), Na (0.3) and K (0.1). The accuracy for the calcium analysis is about +/- 2.5 wt % oxide.

In order to verify the SEM-EDS analyses, the calcium content in the cement paste was determined by EDTA-titration. A sample of the mortar was cut into two halves, each half treated as a separate sample representing an outer and an inner zone. The outer zone had a carbonated layer of about 0.5-1 mm thickness, which was excluded from the analyses. The bulk calcium content in each zone, expressed as wt % CaO, was calculated after a determination of the aggregate content.

To the naked eye, a distinct difference between the outer and the inner zone was observed divided by a fairly sharp boundary. The outer zone, which was facing the water in the tank, had a pale colour and a porous structure. The inner zone, next to the steel confinement, had a dark colour and a dense structure. These observations were later confirmed by microscopy and porosity studies (see Appendix 2 and 3).

The accuracy of the measurement of the calcium content by titration is high, about 0.002 %.

## 3.2 Structural features and distribution of mineral phases

### 3.2.1 Electron microscopy (SEM)

Replacement phenomena in clinker grains, crystallisation of secondary mineral phases in voids, carbonation and dissolution and transportation of water-soluble components in the capillary pore system, are examples of mechanisms, which changed the structure of the cement paste. Such structural changes were identified and analysed by electron microscopy. The result is shown in Appendix 1.

A SEM-EDS point-counting showing the abundance of coarse-grained, recrystallised portlandite or calcite in the cement paste, was also carried out. Portlandite recrystallisation often takes place in clinker grains as replacements of clinker phases or as mineralisations in air-voids. The identification of portlandite and cement gel components was made at constant intervals along traverses throughout a cross section of the concrete mortar in sample 1. The result is shown as the volume percentage of portlandite/calcite in the cement paste (Appendix 1, page 7).

### 3.2.2 Thin section study

The structure and mineralogy of the cement paste was further studied with thin sections in a light transmission microscope. The result is shown in Appendix 2, where microphotographs from a cross section of the concrete mortar are presented.

## 3.3 Porosity

The porosity change in the cement paste was studied in a light transmission microscope with fluorescent light and quantified by an image analyser coupled with SEM.

Images were analysed along traverses at various levels resulting in profiles through the concrete mortar. In sample 1, three different runs were made with the SEM/image analyser and in sample 2, two runs. The magnification and the analysed field area were changed between the runs in order to see the variation in porosity for different pore size ranges. At least 15 analyses from each traverse were made depending on the analysed field area. In sample 1, the range 1-30 microns corresponds with coarse capillary pores, leached clinker grains and air voids and the range 1-10 microns with coarse capillary pores and fine clinker grains and finally 10-30 microns with air voids and coarse clinker grains. In sample 2, the

ranges 200 nanometer - 2 microns and 2-30 microns were analysed, where the former represents the capillary pore system.

The results from fluorescent light microscopy and SEM/image analysis are shown in Appendix 3.

# 4 Results

## 4.1 Element distribution

SEM-EDS analysis of the cement paste from the concrete mortar in the water tank was compared with mean values from 90 Portland cement analyses from 1910. These cement analyses were reported 1923 in Betong, Häfte 1, issued by the Swedish Concrete Association. The cement analyses from 1910 in wt % oxide normalised to 100 % are as follows:

| | $SiO_2$ | $Al_2O_3$ | $Fe_2O_3$ | CaO | $SO_3$ | MgO |
|---|---|---|---|---|---|---|
| Mean value | 23.0 | 6.1 | 2.7 | 64.2 | 1.0 | 2.6 |
| Highest value | 25.0 | 7.8 | 3.9 | 68.2 | 1.2 | 3.1 |
| Lowest value | 21.3 | 4.2 | 2.0 | 62.1 | 0.7 | 0.8 |

The highest acceptable value for $SO_3$ at this time according to Swedish regulations was 2.5 wt %. The $SiO_2$ and CaO values in Portland cement have been very stable over time and are most likely to have been the same in the Portland cement used in the watertank 1906. Also for the other elements, there is no reason to believe that there has been any significant difference between the original cement composition in the watertank and the recorded cement analyses from that time. Total mean values of all analysed points from the concrete mortar in the watertank are shown in the table below for some major elements.

| Profile no. | $SiO_2$ | $Al_2O_3$ | $Fe_2O_3$ | CaO | $SO_3$ | MgO |
|---|---|---|---|---|---|---|
| 1 | 34.1 | 6.0 | 1.9 | 53.6 | 2.6 | 1.1 |
| 2 | 24.6 | 6.0 | 1.3 | 63.4 | 2.2 | 1.9 |

A comparison between the unaltered cement from 1910 and profile 1 and 2 leads to the conclusion that fairly strong calcium depletion has taken place in profile 1. Profile 2 had about the same element contents as the unaltered cement, which suggests that no bulk loss has taken place but the redistribution of the elements within the concrete mortar.

The variation of the different elements in profiles 1 and 2 were as follows (see also diagrams in Appendix 4):

*CaO*

From the water-exposed surface and to about 0.5 mm depth, an excess of calcium compared to normal calcium values in cement at this time was recorded. This zone corresponds to the carbonated zone consisting mostly of calcite. After about 0.5 mm depth, the calcium content gradually decreases and reaches a minimum at about 3-4 mm depth. From this depth an increase takes place and at about 5- 7 mm depth the calcium content stabilises and reaches a constant level (see Appendix 4, page 2, 3, 5, 6, 16 and 18).

In profile 1, the calcium content behind 5 mm depth was about 10 wt. % CaO lower compared with the mean value of 90 cement analyses from 1910. In profile 2, the mean calcium content at these depths was approximately the same as in the cement analysis from 1910. In profile 1, the minimum value in the outer zone (0-7 mm) was about 45 wt. % CaO and the mean value in the inner zone (8-13 mm) about 52 wt. %. In profile 2, the minimum value in the outer zone (0-7 mm) was about 50 wt. % and the mean value in the inner zone (8-18 mm) about 60 wt. %.

The analyses of the calcium content by EDTA-titration and by determination of the aggregate content gave a result similar to profile 1. After stripping of 1 mm from the surface (carbonated zone), the outer zone (1-7 mm) had about 45 wt % CaO and the inner zone (8-18 mm) had about 50 wt % CaO.

*$SiO_2$ and CaO/$SiO_2$-ratio*

The variation in silica concentration mirrors the variation in calcium content, which is taken as evidence for silica immobility (Appendix 4, page 4, 5, and 17). This was confirmed by comparing the bulk contents of CaO + $SiO_2$ in profile 1, profile 2 and the cement analysis from 1910 (see tables in section 3.1). The sum was identical in all three cements and the ratio 1/CaO + $SiO_2$ did not vary through profiles 1 and 2.

*$Al_2O_3$*

From the surface and to about 1 mm depth the aluminium concentration was low. This zone is the carbonated zone dominated by secondary calcite formation. From 1-2 mm depth, aluminium had a peak in both profiles indicating ettringite formation. After 2 mm depth in profile 1, aluminium fluctuates with highs and lows around the mean value given by the cement analyses from 1910. A combination of high concentrations in both aluminium and sulphate indicate ettringite and probably thaumasite formation.

The variation of aluminium was somewhat different in profile no. 2. After the peak at about 1 mm depth, aluminium stabilised near the mean value from the reference cement analyses, which indicated that ettringite formation due to water movements in the capillary pore system had taken place in a smaller scale.

The variation of the aluminium concentration is shown in Appendix 4, page 7, 8 and 19.

*$SO_3$*

Similar to the aluminium variation, the sulphate concentration was low in the carbonated zone and had a peak at about 2 mm depth. In both profiles, the sulphate concentration dropped to about the same level as the highest acceptable value in cement from 1910 at about 7 mm depth, which corresponds to the approximate boundary between the outer and inner zones. As previously mentioned, this suggests that there is a clear correlation between calcium depletion (Appendix 4, page 4 and 16) and high concentrations of sulphates and aluminium (page 7, 9, 19 and 20). Redistribution of sulphates and aluminium in calcium depleted areas lead to secondary formation of ettringite, monosulfate and probably thaumasite. These minerals consist primarily of Ca, Al and $SO_4^{2-}$. Some iron may also substitute for aluminium in ettringite phases. The existence of ettringite was confirmed by electron microscopy.

Profile 2 showed a decrease in sulphate concentrations to the same level as the mean value in cement from 1910 at about 12 mm depth. This indicated very small water movements in the inner zone in profile 2, while the inner zone in profile 1 seems to have been subjected to stronger water movements.
The variation in sulphate concentration is shown in Appendix 4, page 9, 10 and 20

*$K_2O$ and $Na_2O$*

In both profiles, a certain enrichment of sodium existed from the surface to about 1 mm depth (carbonated zone). At deeper levels sodium dropped to non-detectable amounts.

Potassium behaved in a similar way and is somewhat enriched to about 1 mm depth. However, at deeper levels potassium fluctuated near the mean value of the cement analyses from 1910.

The variation in sodium and potassium concentrations is shown in Appendix 4, page 12, 13, 22 and 23.

*MgO*

The distribution of magnesium shows a somewhat erratic pattern. Generally, the magnesium concentration seems to be low compared with the mean value of the 90 cement analyses from 1910, indicating depletion. The precipitated crust on the water exposed surface contained high amounts of magnesium compared with the cement in the concrete mortar (see Appendix 1, page 6).

The variation in magnesium concentration is shown in Appendix 4, page 11 and 21.

*$Fe_2O_3$*

Fe is more or less an immobile element in cement materials due to its low solubility. However, iron can substitute for aluminium in ettringite, which is indicated by the coincident distribution pattern of $Fe_2O_3$, $Al_2O_3$ and $SO_3$ (see Appendix 4, page 7, 9, 14 and 19, 20, 24). These elements form a peak at about 1-4 mm, which coincides with the abundant ettringite formation at depths of about 2-3 mm (see Table 1, Appendix 1).

Notably, this also coincides with a low calcium content, indicating more or less "in situ" formation of ettringite where calcium is depleted. As mentioned previously, the level of particularly sulphate seems to reflect remobilization (depletion/enrichment) of calcium in the profiles.

The variation in iron concentration is shown in Appendix 4, page 14 and 24.

## 4.2 Structural features and distribution of mineral phases

On the water exposed surface, a crust of precipitated calcium and manganese carbonate exists. The crust was analysed and the result is shown in Appendix 1, Table 2. Manganese is probably derived from the drinking water and calcium from the cement paste. The outermost 0- 1 mm of the concrete mortar has been carbonated and contains about 75-90 wt % CaO. This zone is dominated by calcite.

Behind the carbonated zone and to about 4 mm depth, the cement paste has been coarsened showing a "sugar-like" grainy texture of recrystallised portlandite crystals and abundant ettringite formation (see Appendix 2, page 2). This is coincident with a drop in calcium content which occurs from about 1-2 mm to 4 mm. A striking feature in this zone is the many empty clinker grains, which have been leached out. The remaining voids have sharp angular walls indicating former alite grains or "spotty" half-empty grains with blurred boundaries indicating former belite crystals. This is shown in Appendix 1, page 2, 3 and 4. Some of the voids have been partially filled with portlandite and ettringite.

From about 4 mm to about 8 mm the cement paste has been heavily leached resulting in numerous large voids with irregular and "channel-like" shapes. This is shown in Appendix 2, page 3, 4 and 5. This zone can be interpreted as a leaching front.

At about 8-9 mm, marking the end of the leaching front, numerous "ring-structures" exist in former air-voids. The rings consist of alternating portlandite and ettringite crystallisation, which marks changes in fluid composition and episodes of precipitation. Precipitation started along the walls of the air-voids and the initial precipitates always consist of portlandite. Portlandite crystallisation was followed by a thin layer of ettringite crystallisation. After these two fairly pure and differentiated zones an inner core with mixed portlandite and ettringite crystallisation exists which sometimes was followed by one more ettringite layer. At the most, up to 5-6 layers were observed. Evidence of "ring-structures" at 8 mm depth is shown in Appendix 2, page 8.

Behind this zone and to the steel confinement, the cement paste becomes denser which is indicated by the dark colour under the polarising microscope (see Appendix 2, page 5, 6 and 7). This also indicates that the cement paste in the inner part of the concrete mortar has been left, if not unaltered, at least much less altered by migrating fluids. This was supported by porosity measurements with a SEM-coupled image analyser shown in Appendix 3.

The distribution of portlandite and calcite in the cement paste was determined through a cross section by SEM analyses in points along traverses and the result is shown in Appendix 1, page 7, as volume % portlandite of paste. The result shows that a narrow zone up to about 1 mm from the water exposed surface is dominated by calcite (carbonated zone). Compared with a mean volume % of calcium hydroxide in modern paste, with a similar water-cement ratio, the concrete mortar in the water tank shows a depletion in portlandite content to a depth of about 8 mm. In a narrow zone between 8-10 mm a marked increase in portlandite content occurs, which is coincident with the zone displaying the "ring-structures".

Next to the steel confinement at 13 mm depth, the paste has been carbonated which may explain the slightly lower portlandite content between 10 and 12 mm depth.

Results of structural and mineralogical observations from SEM and thin section studies are shown in Appendix 1 and 2.

### 4.3 Porosity

Results from porosity measurements by SEM-coupled image analysis are shown in Appendix 3, page 4-8. Three different porosity measurements were made in profile 1 and two in profile 2. The size of the analysed field and the magnification was changed between the measurements in order to detect the variation of different pore size ranges.

The porosity variation for the pore sizes 1-30 and 1-10 microns in profile 1 show a similar pattern. The cement paste showed a decreased porosity in the outermost carbonated zone (0-1 mm) which is followed by an increase to a depth of about 7-8 mm indicating the position of a leaching front. Behind this depth, the cement paste becomes dense.

The porosity variation of the coarser pore size range of 10-30 microns showed a marked increase between 4 and 7 mm defining the zone with heavy leaching and coarse pores which was also observed under the polarising light microscope (see Appendix 2, page 4).
The porosity in profile 2 showed a similar variation but the porosity dropped already at about 4 mm depth.

The porosity variation was further studied under a fluorescent light microscope and photographs are shown in Appendix 3, page 1-3. These observations correspond with the results from the image analysis.

## 5 Summary of results

The results from the investigation is summarised as follows:

- Distribution of some major elements along two profiles was determined by SEM-EDS analysis. Analysis from profile 1 showed that the whole sample has been affected by calcium depletion. Mean values from all the calcium analyses in profile 1 and 2 showed that the sample in profile 1 has lost about 10 wt % CaO compared with profile 2. Also compared with unaltered cement from 1910, the sample in profile 1 shows a loss of about 10 wt % CaO.

The total mean value from calcium analysis in profile 2 was found to be the same as in the recorded cement analysis from 1910. This indicates that the bulk calcium content in sample 2 has not been changed but that mere internal redistribution of calcium has taken place.

- Behind the carbonated zone, both profiles showed a marked decreasing calcium content to depths of about 5-8 mm. Behind this depth the calcium content stabilised at a higher level, indicating a leaching front at about 8 mm. However, in contradiction to profile 2, the stabilised calcium level behind 8 mm in profile 1 is low, indicating calcium depletion through the whole profile in sample 1.

Further determination of the bulk calcium content by EDTA-titration gave a result similar to the SEM-EDS analysis in profile 1. A sample was split into two halves, one representing the outer zone (1-8 mm) and the other the inner zone (9-18 mm). SEM-EDS and EDTA-titration showed the same result in decreased bulk calcium content.

- The marked calcium depletion between the carbonated zone and to depths of 5-8 mm corresponds with a relative increase in the sulphate, iron and aluminium concentrations. The apparent increase of these elements is a consequence of calcium depletion rather than true enrichment and reflects the abundant ettringite crystallisation, which was observed in this zone. The diagram below illustrates the relative changes in element concentrations due to calcium depletion and subsequent ettringite crystallisation in profile 1.

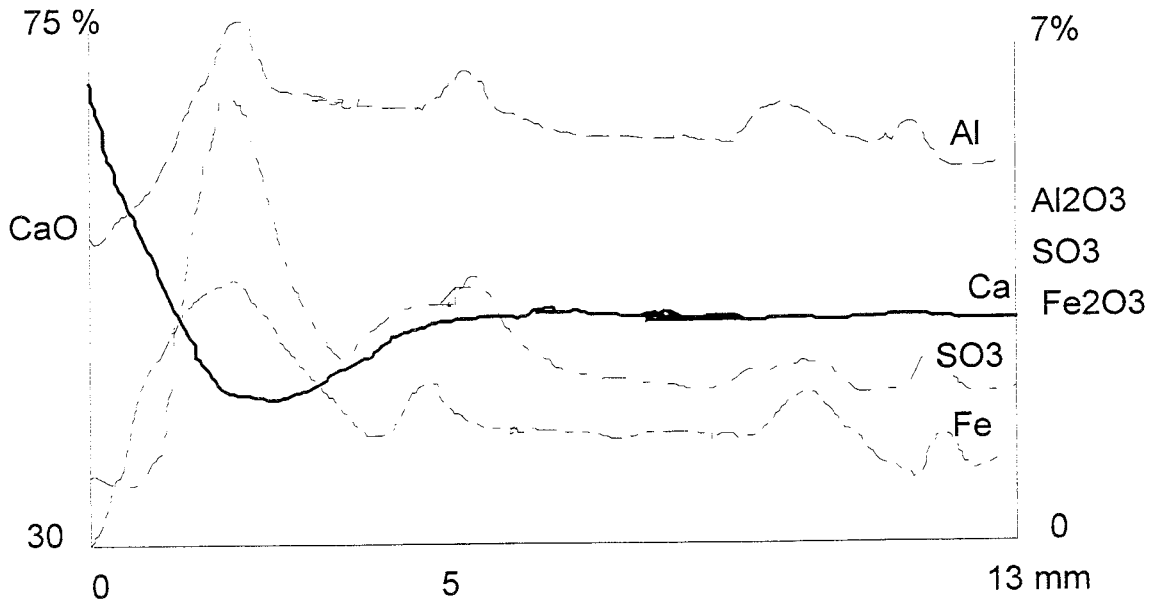

- The sum of $CaO + SiO_2$ was exactly the same in profile 1, profile 2 and in the cement analysis from 1910. This suggests that silica essentially behaved as an immobile element during calcium depletion. The relative changes in silica concentration through both profiles exactly mirrors the changes in calcium contents.

- Potassium and sodium was enriched in the carbonated zone. At deeper levels sodium has been depleted, dropping to the non detectable limit, while potassium stabilised at the same level as the mean value of cement analysis from 1910.

- The only significant bulk loss from the samples was calcium in profile 1. The other elements seem to have been more or less redistributed within the concrete mortar. Sulphate aluminium and iron were included in new mineral phases. Sodium and potassium were to some extent trapped in the carbonated zone.

- Mineralogical changes have taken place in the cement paste due to dissolution, migration and precipitation. Examples of such changes are dissolution of old clinker phases and precipitation of calcium and sulphate-bearing phases such as portlandite, ettringite and thaumasite. Secondarily formed calcium silicate hydrates (C-S-H phases) with a calcium: silica ratio of about 1:1, was observed in spaces after former clinker grains.

Carbonation of calcium hydroxide next to the water-exposed surface has lead to calcite formation. Calcite formation probably led to further calcium depletion behind the carbonated zone by migration of calcium hydroxide. This eventually formed the somewhat more dense and calcium-enriched carbonated zone.

Calcite together with manganese carbonate also formed a crust on the water-exposed surface itself.

- Porosity measurements with a SEM-coupled image analyser showed an increased fine porosity behind the carbonated zone to about 7 mm depth in profile 1 and about 4 mm in profile 2. This is in accordance with the marked calcium depletion/leaching front found by SEM-EDS analysis. The carbonated zone showed a lower porosity.

Measurements of the coarser pore sizes showed a marked increase between 4 and 7 mm.
The result from the image analysis was confirmed by fluorescent/polarising light microscopy of thin sections. A somewhat denser carbonated zone was followed by an increased fine

porosity to depths of about 3-4 mm and a zone with coarse porosity to about 9 mm depth. Behind this depth the cement paste becomes dark and denser.

## 6 Discussion

Hydrated cement paste is a porous medium whose solid phases are stable at a very basic pH. The solid phases are in contact with a pore solution dominated by alkali, calcium and hydroxide ions. The amount of alkalis is limited and they leach very easily. Thus the leaching is mainly controlled by the solubility and buffering effect of calciumhydroxide (CH). When the CH is consumed, the calciumsilicatehydrate (C-S-H) ettringite/monosulphate becomes unstable and the cement paste disintegrates.

The leaching rate is also controlled by the permeability and the ability for water to pass through the mortar concrete. In the water tank, the water can not pass through the mortar. Thus the dissolution will be diffusion-controlled.

The mortar from the water tank shows that CH still remains in most of the samples although it has been leached for more than 80 years. The result shows that diffusion-controlled leaching is slower than expected. The leaching of CH has often been calculated according to the "shrinking core model". It can be instructive to calculate the expected depletion of CH according to this model. Assuming the instantaneous release of leachate from the inner surface of the water tank to the fresh water, the following equation (according to Höglund et al. 1991) can be used:

$$X=(2D_e c_s t/q_0)^{1/2}$$

Where x is the penetration depth, $D_e$ the effective diffusivity in leached concrete, $c_s$ the solubility of CH, t the time and $q_0$ the initial amount of CH in the mortar. Parameter values, suggested by Höglund et al. (1991) and used performance assessment of repository constructions, are, $D_e = 3x10^{-11}$ $m^2/s$ and $c_s$=25 $mol/m^3$. The content of CH is estimated to be around 1150 $mol/ m^3$.

If it is assumed that all these values are applicable to the water tank, the penetration depth after 90 years can be calculated at around 6 cm, which is significantly more than what can be observed. According to this calculation, no portlandite should remain. The portlandite depletion is at least a factor of 10 less than previously assumed in performance assessments of repository constructions.

This may be due to several factors. The carbonation of the outermost layers may delay the ion exchange. The most plausible explanation is, however, probably that the shrinking core model does not consider alteration processes in the cement matrix. The leaching process is more complicated than assumed. The shrinking core model assumes that portlandite is removed which increase the porosity. The mortar from the water tank shows that, given time, the paste does not only lose CH but adjusts itself by modifying the C-S-H, hydration of remaining clinker grains and recrystallization of ettringite/monosulphate. Leaching tests will not show these phenomenas as the time period for the experiments normally are too short.

# 7 References

Höglund, L. O., and Bengtsson, A., 1991, Some chemical and physical processes related to the long-term performance of the SFR repoitory, SFR Prog. Rep. 91-06, Stockholm Sweden.

Lagerblad, B. and Trägårdh, J.1994, Conceptual model for concrete long time degradation in a deep nuclear waste repository. SKB Tech. Rep. (TR 95-21), Stockholm Sweden.

Lagerblad, B., 1996, Conceptual model for deterioration of Portland cement concrete in water, SKB Prog. Rep.

# Contents of Appendixes


| | Page |
|---|---|
| Appendix 1- Structural features (SEM) | 1-7 |
| Photograph showing analysed points in sample 1 | 1 |
| Structural features in the outer zone | 2 |
| SEM-micrographs showing some structural features | 3-4 |
| Table 1. Structural observations along a crossection | 5 |
| Table 2 and 3. Chemical composition of major clinker phases and products precipitated on the surface | 6 |
| Table 4. Distribution of portlandite and calcite along a crossection | 7 |
| Appendix 2- Structural features (Thin section) | 1-8 |
| Photograph of polished piece | 1 |
| Photographs with polarised light, crossection | 2-7 |
| Photograph of "ring-structures" | 8 |
| Appendix 3- Porosity | 1-8 |
| Photographs with flourescent light, crossection | 1-3 |
| Porosity from image analysis, sample 1 | 4-6 |
| Porosity from image analysis, sample 2 | 7-8 |
| Appendix 4- Element distribution | 1-24 |
| Major element distribution in sample 1 | 1-14 |
| Major element distribution in sample 2 | 15-24 |

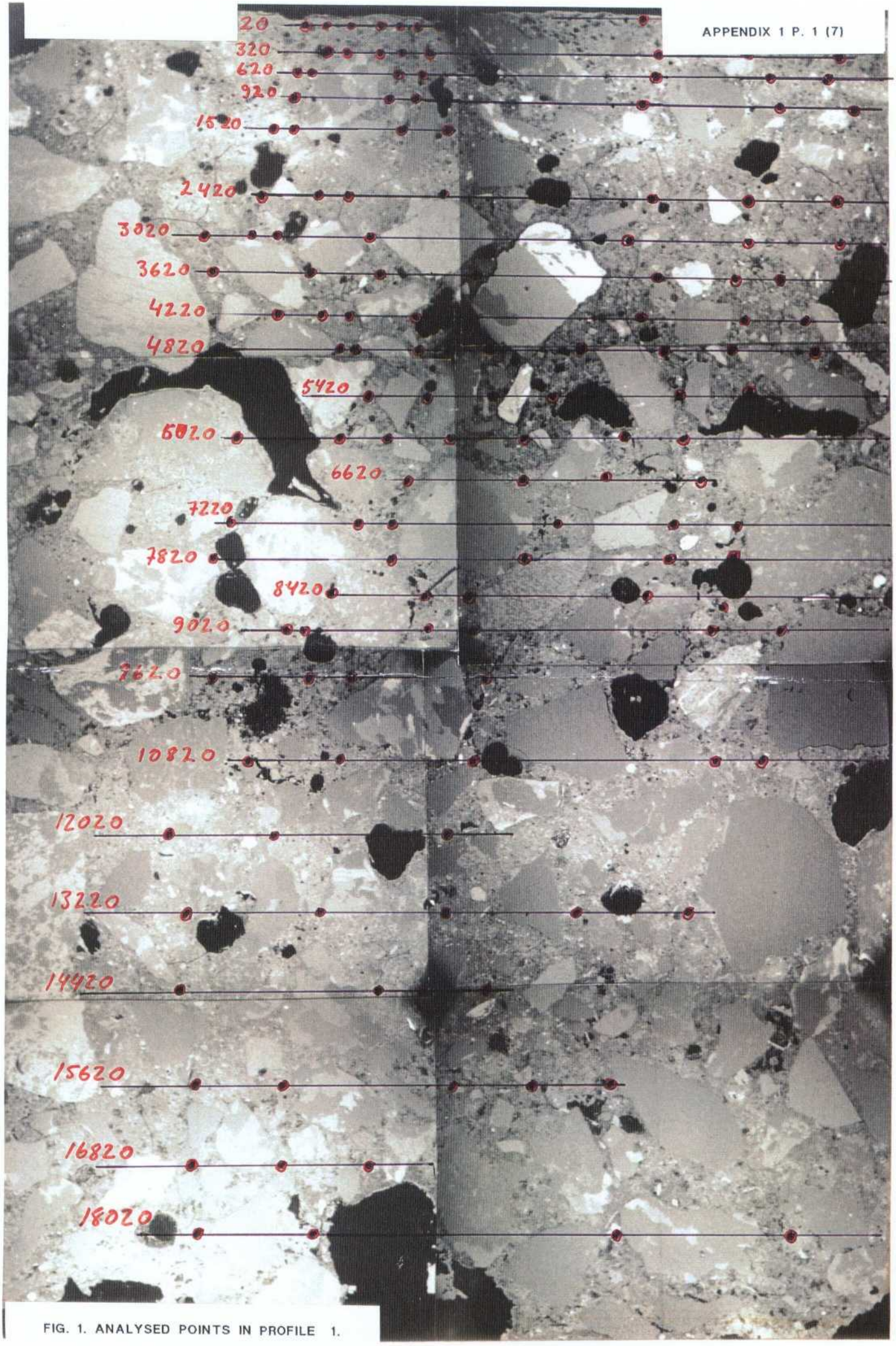


FIG. 1. ANALYSED POINTS IN PROFILE 1.

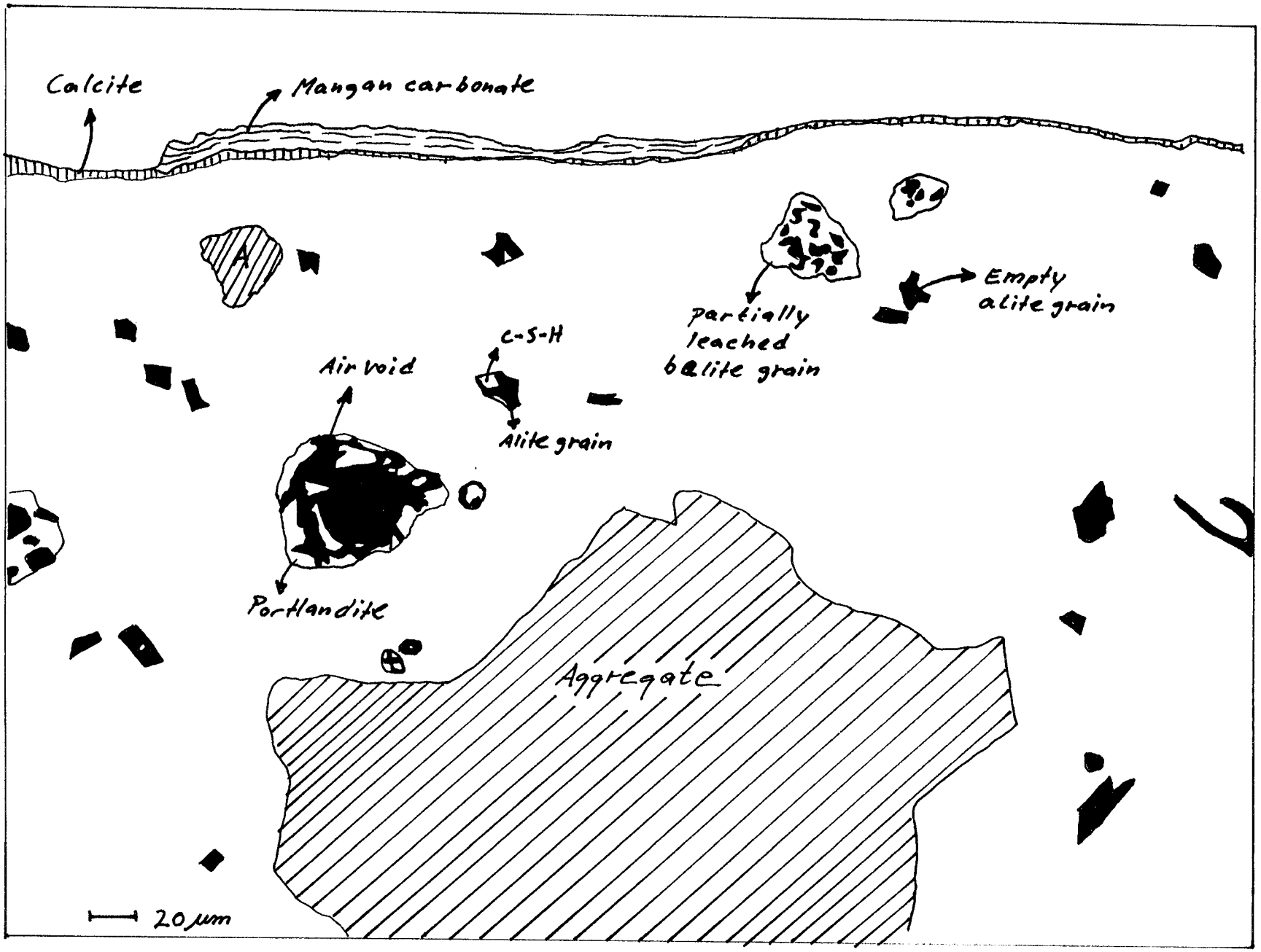


FIG. 2. Structural features in the outer zone (waterside) of the concrete mortar.

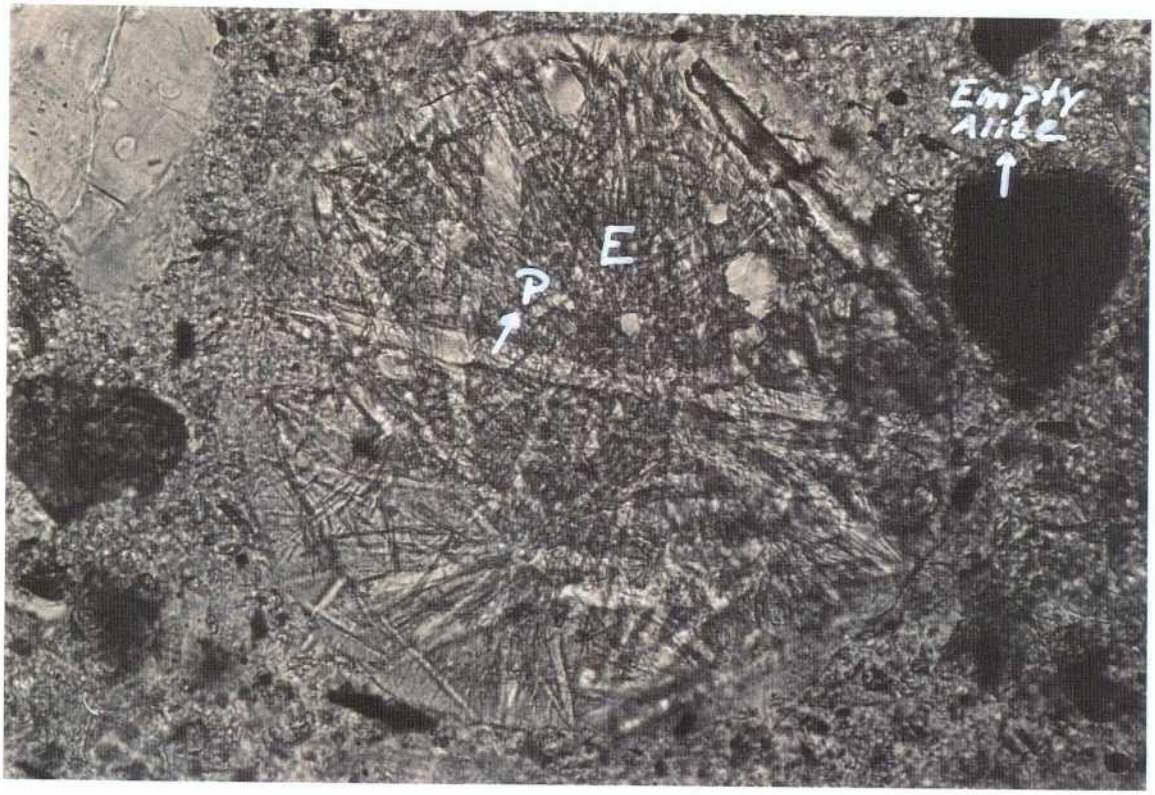


Fig 3. Air-void filled with platy portlandite crystals and needle-like ettringite crystals. Empty alite grain (leached) on the right side.

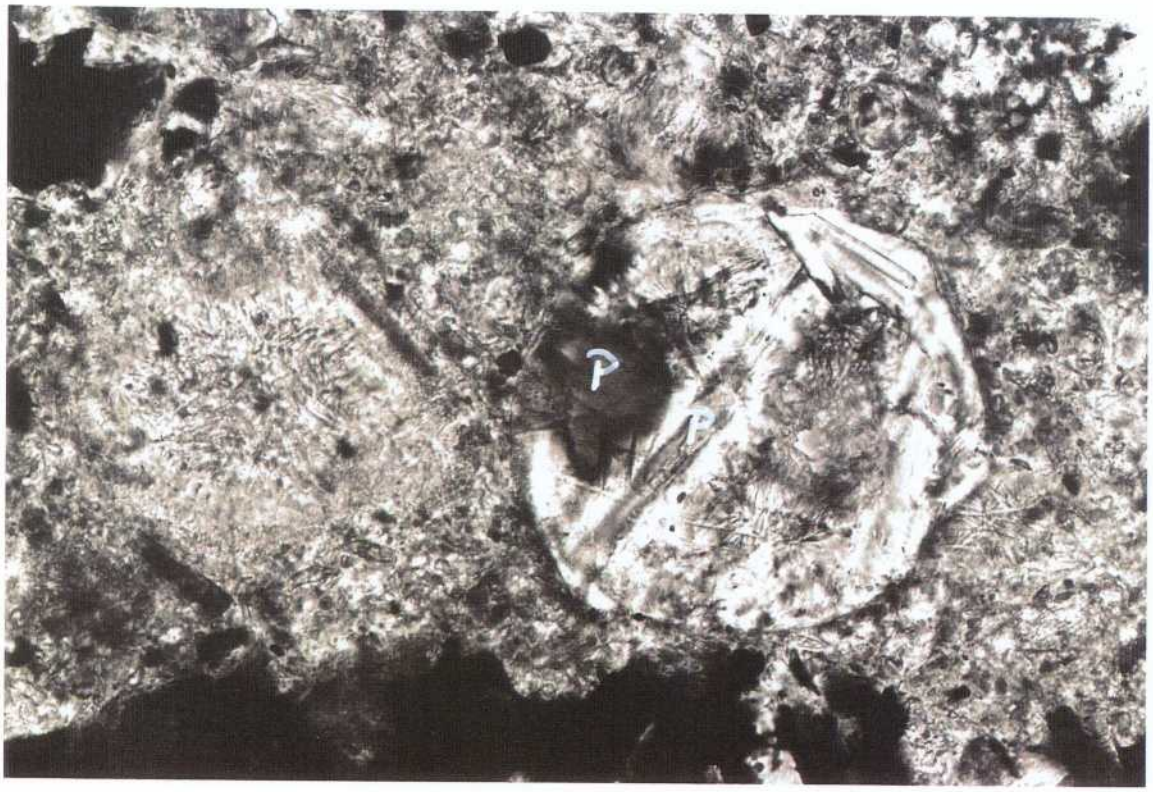


Fig 4. Air-void filled with portlandite.

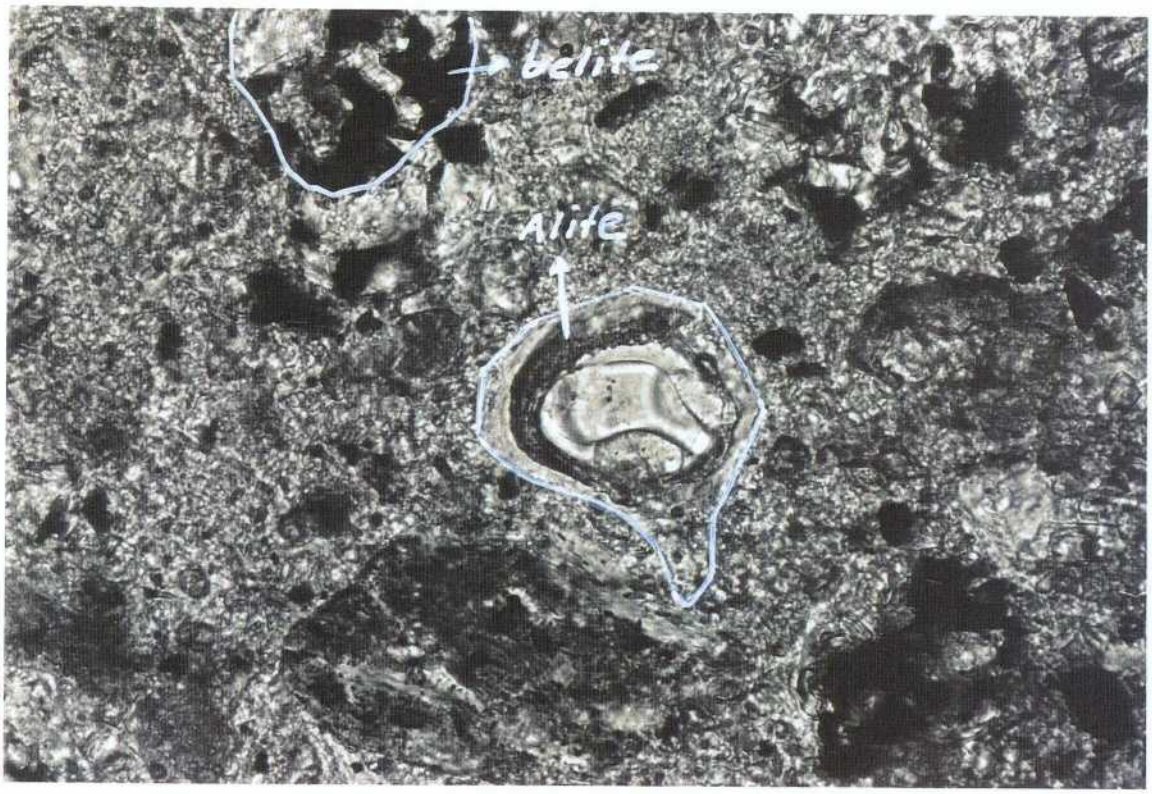


Fig 5. Half-filled alite grain and partially leached belite grain.

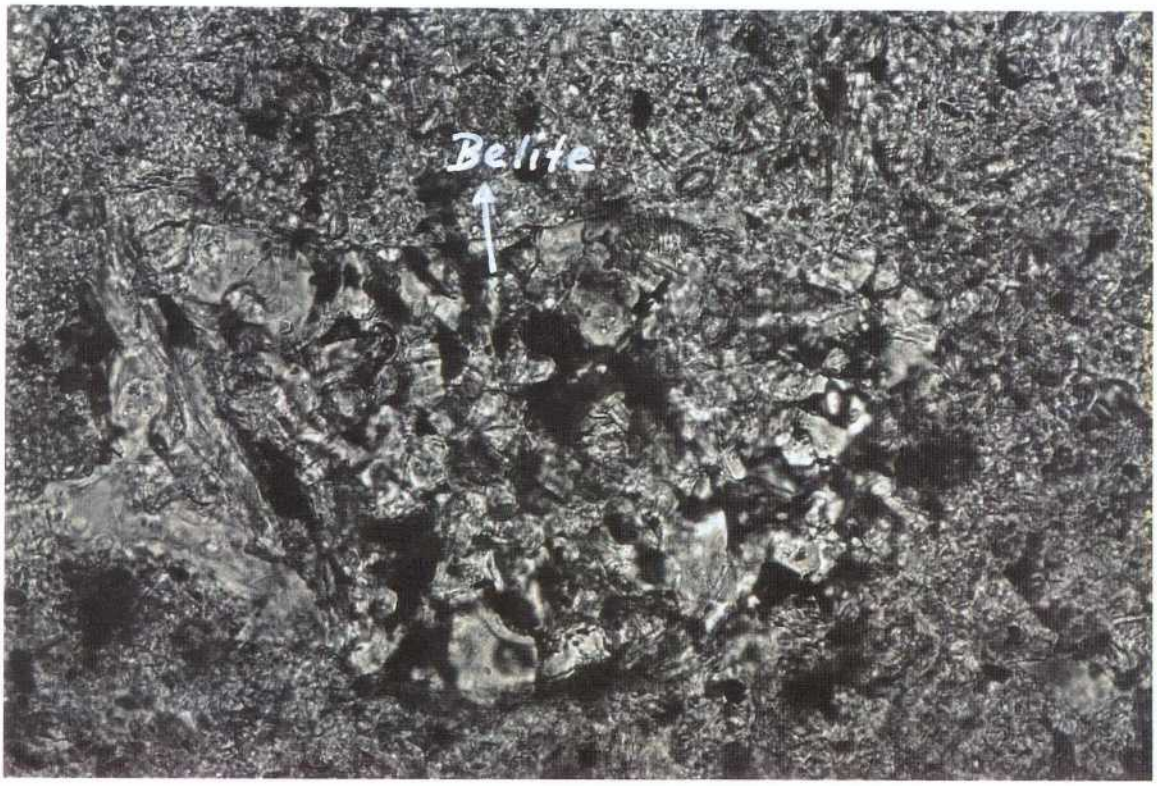


Fig 6. Partially leached belite grain.

**Table 1. Observation from SEM-study of sample no.1**

| Depth (microns) | Observation |
|---|---|
| Surface | Crust consisting of mangancarbonate containing minor calcite (MnCO3 +/- CaCO3). For chemical analysis see Table 2. |
| Edge | Calcite. For chemical analysis see Table 2. |
| 360 | Dense gel structure but porous clinker grains. Leached alite grains (empty) in the size fraction minus 20 microns. Calcite in air voids. |
| 720 | Dense gel structure but porous clinker grains. Leached alite grains (empty) in the size fraction minus 20 microns. Calcite in air voids. |
| 1080 | Dense gel structure but porous clinker grains. Leached alite grains (empty) in the size fraction minus 20 microns. |
| 1440 | Dense gel structure but porous clinker grains. Leached alite grains (empty) in the size fraction minus 20 microns. |
| 1800 | Dense gel structure but porous clinker grains. Leached alite grains (empty) in the size fraction minus 20 microns. |
| 2160 | Porous structure. Ettringite in voids |
| 2520 | Coarse porous stucture. Pseudomorphs showing "Hollow-shell" structure in old alite grains. The alite grains are often half-filled with an outer rim of C-S-H product and an empty core (Ca/Si-ratio approx. 1:1). Ettringite in voids. |
| 2880 | Coarse porous structure. Ettringite in voids. |
| 3240 | Mixed dense and porous structure. Pseudomorphs as in 3000 level. |
| 3600 | Mixed dense and porous structure. Empty clinker grain. |
| 4000 | Porous structure. Empty clinker grain. Pseudomorph. |
| 4320 | Mixed dense and porous structure. Pseudomorphs as in 3000 level. |
| 4700 | Porous structure. |
| 5040 | Dense gel structure. Empty clinker grains and pseudomorphs with only a thin shell of C-S-H product. |
| 5760 | Mixed dense and slightly porous structure. |
| 6120 | Mixed dense and slightly porous structure |
| 6500 | Mixed dense and slightly porous structure |
| 6840 | Mixed dense and slightly porous structure |
| 8000 | Mixed dense and slightly porous structure. Porous in the coarse side of clinker grain fraction (> 10 microns, empty clinker grains). |
| 8640 | Mixed dense and slightly porous structure. |
| 9360 | Mixed dense and slightly porous structure. Replacement in belite crystal: Portlandite and C-S-H products in lamellae structure and calciumaluminiumsulphate phases in bulk crystal. |
| 10440 | Dense structure. |
| 11160 | Coarse porous structure. Partly leached belite crystals. |
| 11880 | Porous structure. |
| 12960 | Coarse porous structure. |

**Table 2. Distribution of elements in products precipitaded on the surface of the concrete mortar.**

| Oxide weight % | Precipitated crust | Edge |
|---|---|---|
| Na2O | 0.9 | 0.9 |
| MgO | 5.0 | 1.3 |
| Al2O3 | 9.0 | - |
| SiO2 | 3.7 | 1.3 |
| P2O5 | 0.7 | - |
| SO3 | 2.0 | - |
| K2O | 1.5 | 0.9 |
| CaO | 11.4 | 96.3 |
| TiO2 | 1.6 | - |
| MnO | 64.1 | - |
| Fe2O3 | - | - |

**Table 3. Typical element distribution in major clinker phases in Portland cement (from Kjellsen et. al.)**

| Oxide weight % | Alite | Belite | Ferrite |
|---|---|---|---|
| Na2O | - | 0.1 | 0.2 |
| MgO | 0.6 | 0.3 | 1.7 |
| Al2O3 | 0.9 | 1.1 | 16.4 |
| SiO2 | 25.0 | 32.0 | 2.5 |
| SO3 | - | 0.2 | - |
| K2O | - | 0,8 | - |
| CaO | 72.4 | 63.7 | 47.1 |
| TiO2 | - | 0.1 | 0.9 |
| Mn2O3 | - | - | 1,2 |
| Fe2O3 | 1.1 | 1.7 | 30.0 |

**Table 4. Distribution of portlandite and calcite in the cement paste determined by SEM-analysis (Mean value from Taylor, 1990). Sample no. 1.**

| Depth (mm) from surface in contact with water | Frequency of portlandite/calcite analysis in paste (%) | Total number of analysed points in paste (C-S-H analysis in bracket) |
|---|---|---|
| 0.1 | 48 (Carbonation,calcite) | 46 (24) |
| 0.9 | 21 Portlandite | 30 (22) |
| 1.8 | 8 Portlandite | 38 (35) |
| 2.7 | 6 Portlandite | 16 (15) |
| 3.6 | 10 Portlandite | 20 (18) |
| 4.5 | 5 Portlandite | 22 (21) |
| 5.4 | 11 Portlandite | 27 (24) |
| 6.3 | 8 Portlandite | 23 (21) |
| 7.2 | 11 Portlandite | 27 (24) |
| 8.1 | 6 Portlandite | 30 (28) |
| 9.0 | 24 Portlandite | 34 (26) |
| 9.9 | 23 Portlandite | 31 (24) |
| 10.8 | 11 Portlandite | 37 (33) |
| 11.7 | 11 Portlandite | 27 (24) |
| 12.6 | 19 (Carbonation,calcite) | 27 (22) |
| **Total no. of analysed points** | | **435** |
| **Mean vol. % of calciumhydroxide in paste, W/C ratio=0,40** | **18** | |

**Thin section study**

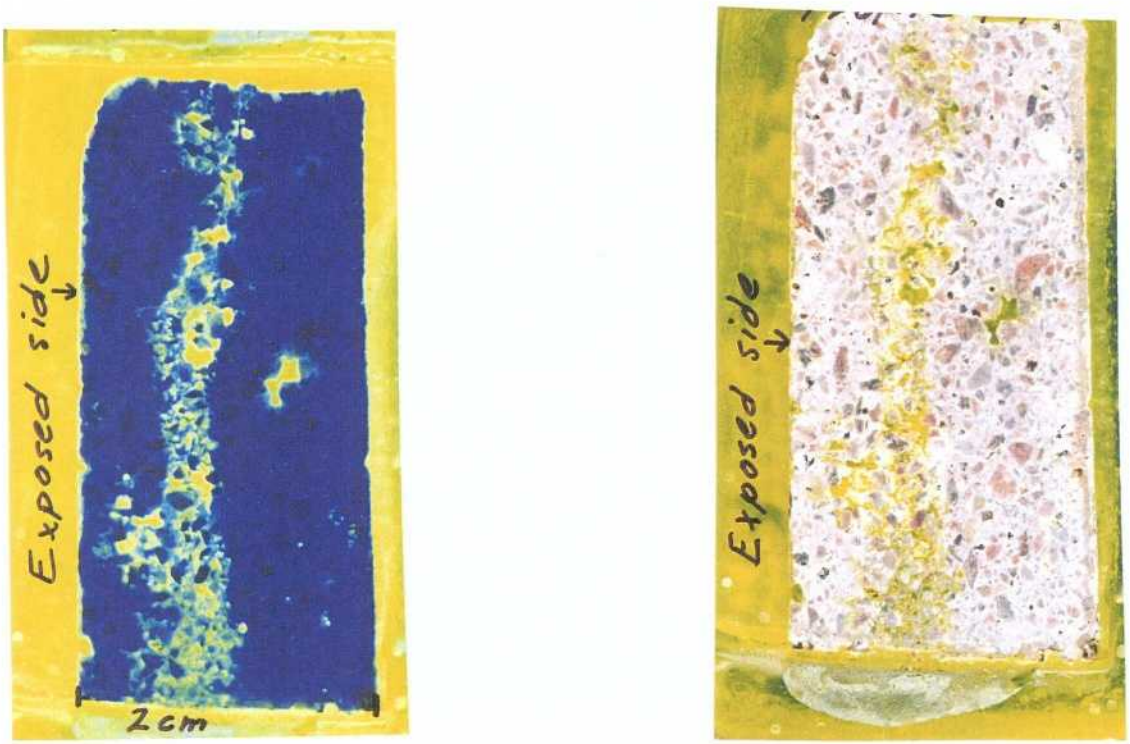


Fig 1. Polished crossection of the concrete mortar in watertank. The sample is impregnated with epoxi with fluorescent dye which reveales the coarse porosity (yellow patches) under fluorescent light. Thin sections were made from the same piece.

**Photographs from thin sections:Level 0-2,6 mm.**

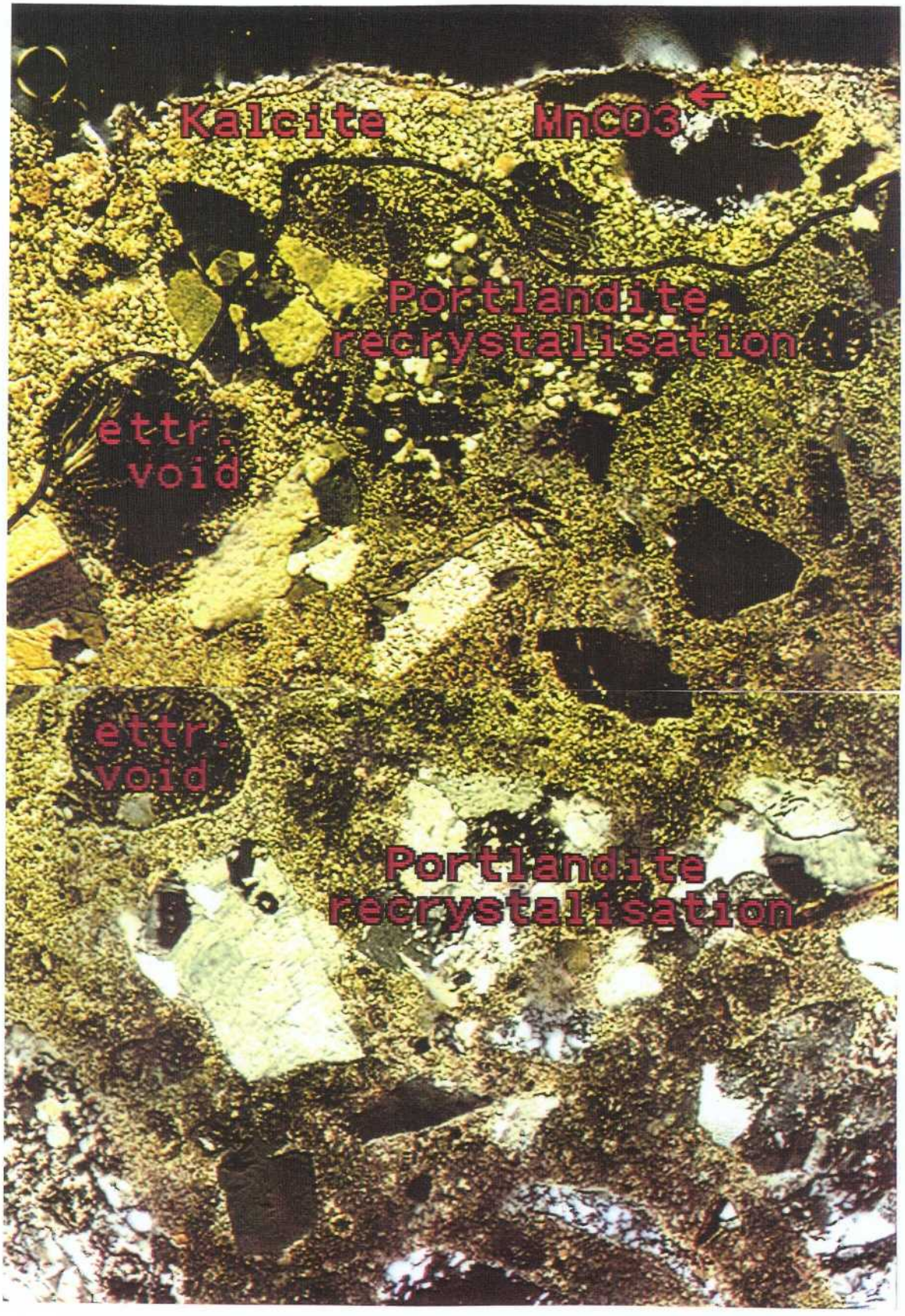


Surface

Calcite Carbonation zone

0,5 mm

Zone with portlandite and ettringite crystallisation (coarsening of cementpaste)

2 mm

-- 2,6 mm depth

Fig 2. Upper carbonated zone containing calcite, 0,5 – 1 mm thick. Abundant portlandite crystallisation from 0,5 mm – 3 mm depth. (Yellowish-grainy areas). Ettringgite-filled circular air voids exist at about 1,5 mm depth.

**Level 2,6-5,3 mm**

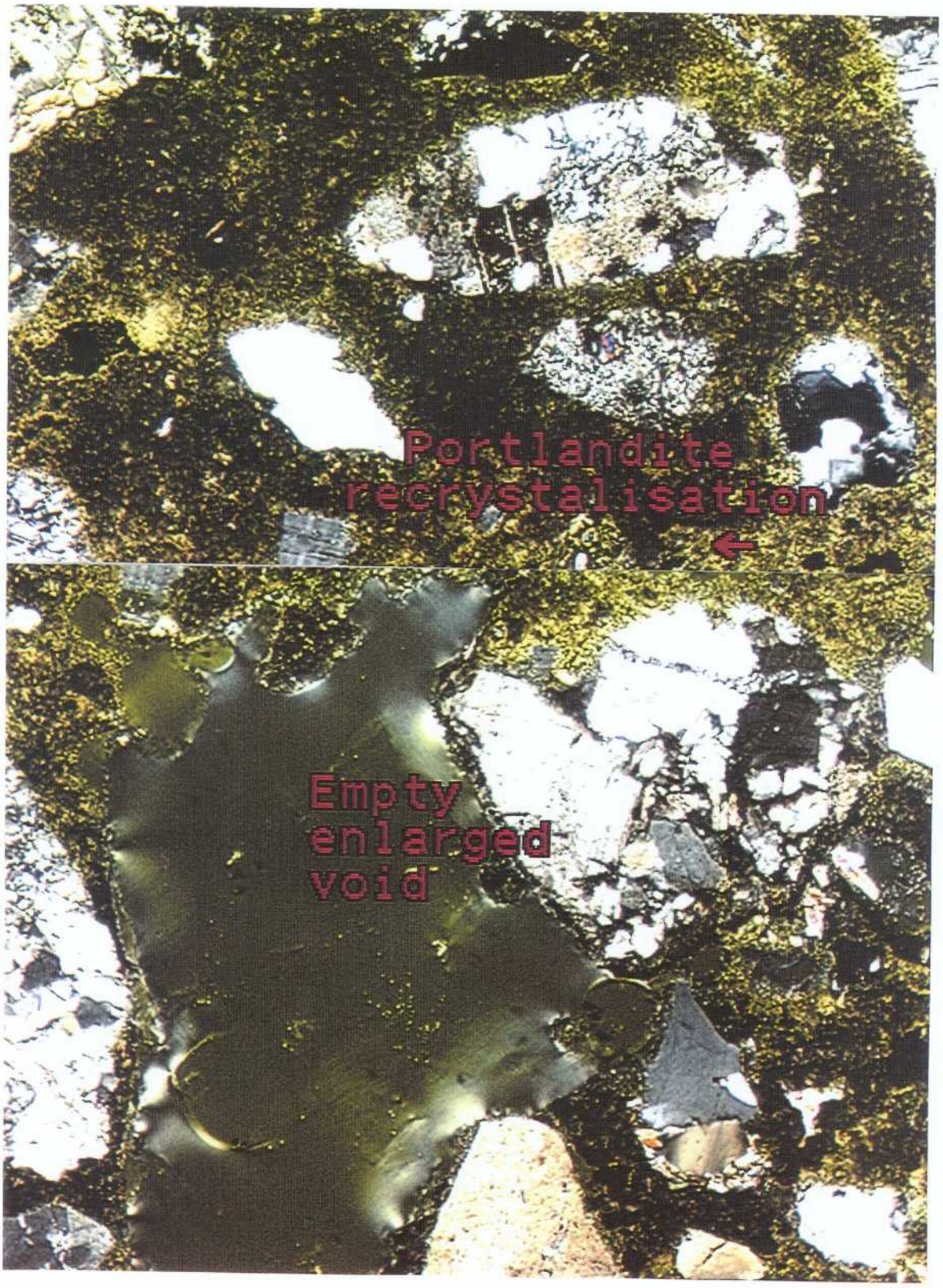


Fig 3. Portlandite crystallisation in patches indicated by "yellowish grainy" areas. At about 4,5 mm depth, a coarse porosity is observed shown by numerous enlarged and irregular air-voids.

**Level 5,3-7,8 mm**

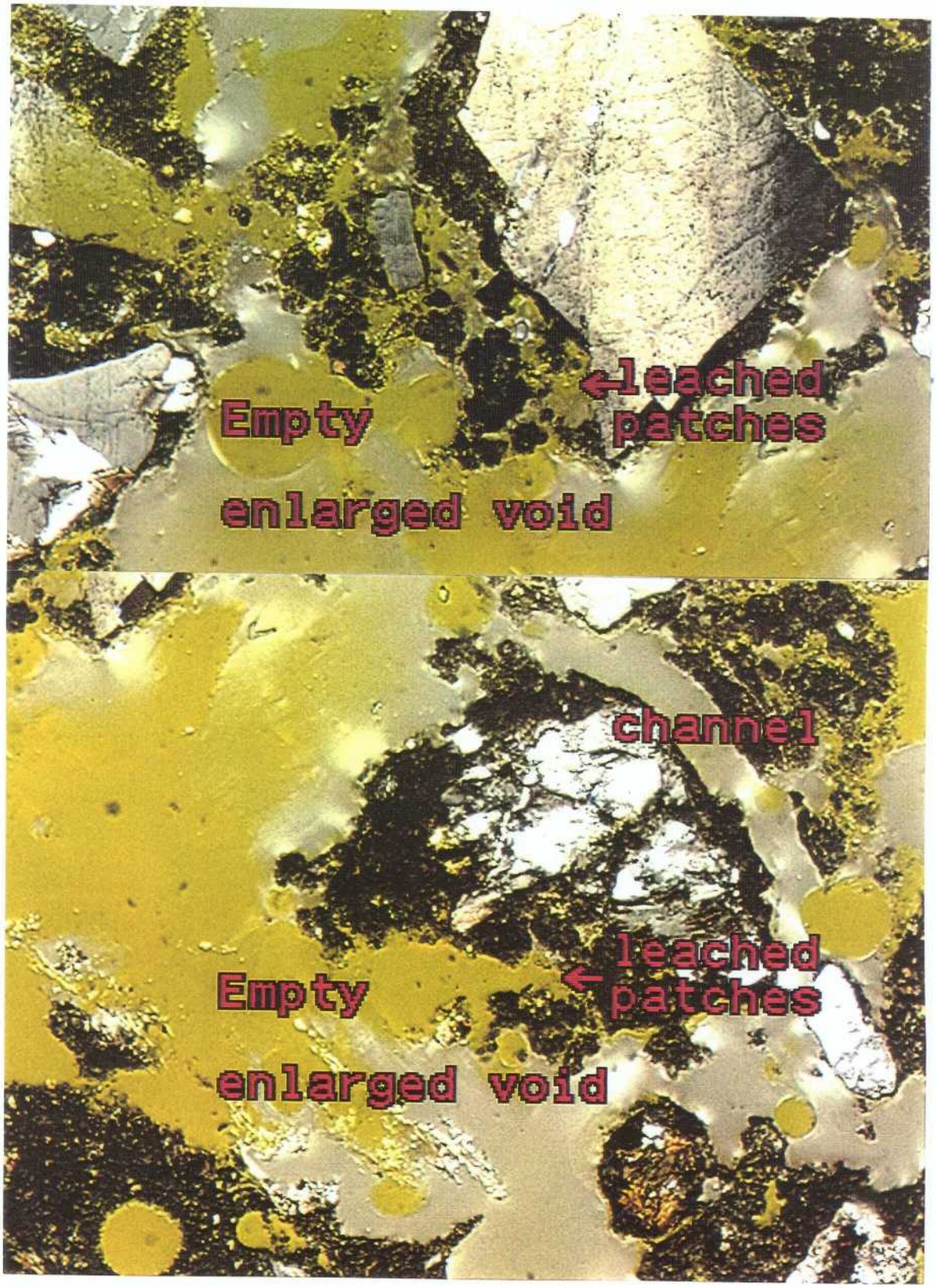


--5.3 mm

Zone with coarse Porosity and leached paste structure

7,8 mm

Fig 4.Zone with coarse porosity shown by numerous enlarged and irregular air-voids. Leached patches in the cementpaste exist at about 7 mm.

**Level 7,8-10,7 mm**

--7,8 mm

Zone with dark cement paste

--10,7 mm

Fig 5. Zone with low porosity and dark cement paste. The structure of the cement paste is less affected by remobilasation and recrystallisation.

**Level 10,7-14 mm**

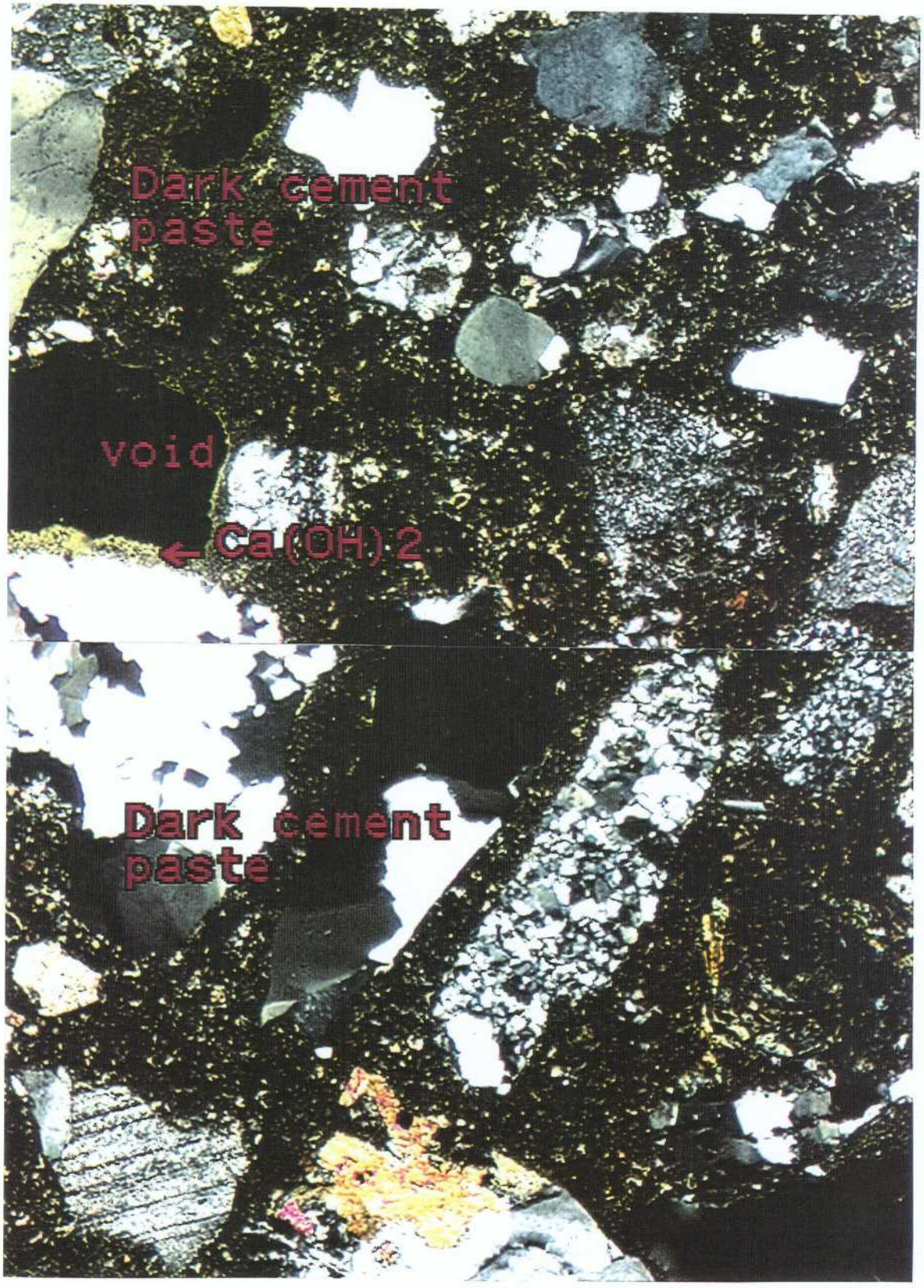


Fig 6. Zone with dark cement paste.

**Level 14-17 mm**

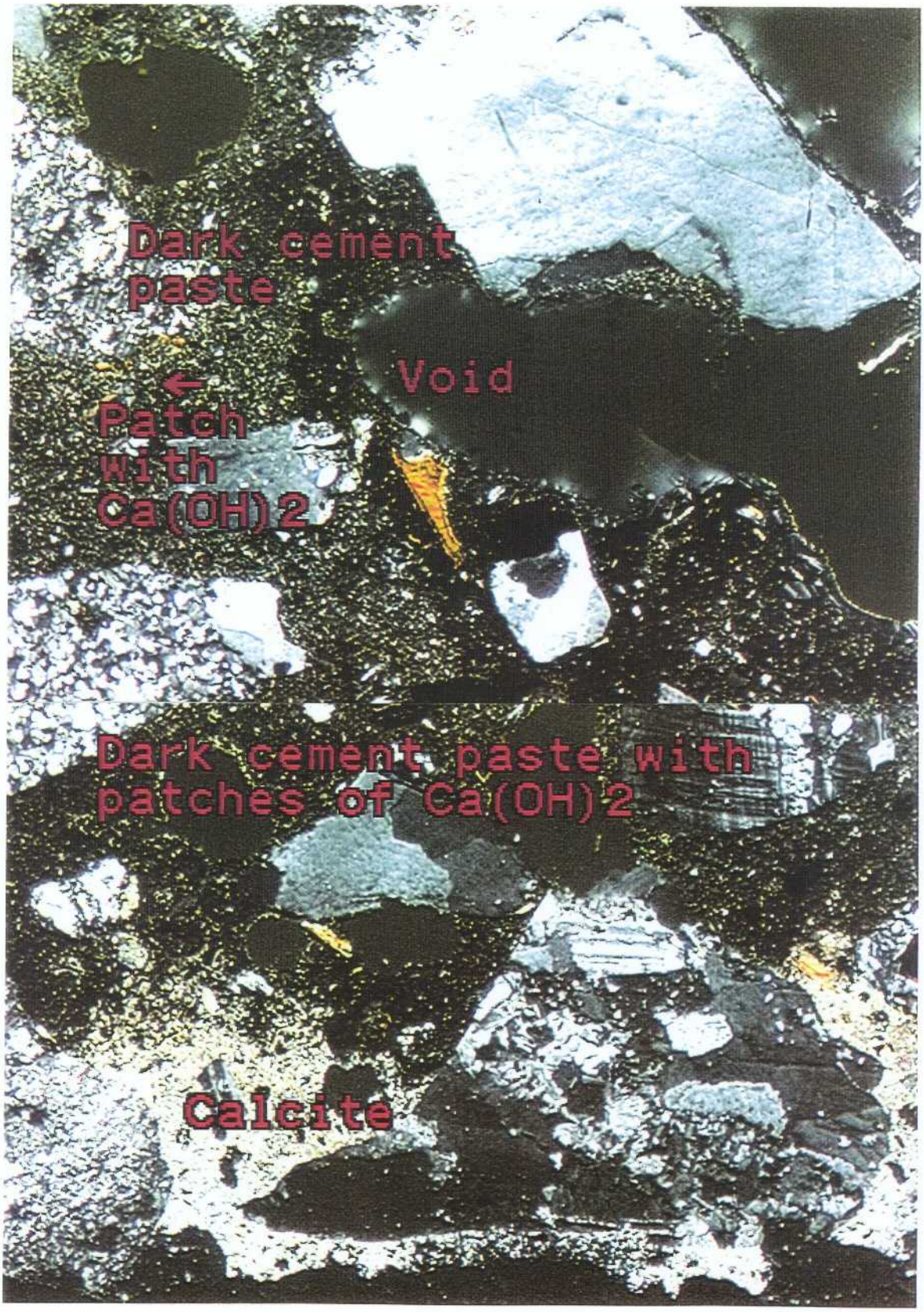


--14 mm

--17 mm

Fig 7. Zone with dark cement paste. Minor patches with portlandite crystallisation.

**Zone with ring structures between zones with portlandite crystallisation and coarse porosity at about 8 mm depth.**

Fig 8. In and just above the zone which is dominated by coarse porosity, numerous portlandite and ettringite-filled air-voids exist. These indicate strong remobilasation of calcium and sulfates. Note the "ring structures" which indicate different epiosodes of precipitation. Dark rings represent ettringite/monosulfate crystals and light-yellowish rings consist of portlandite.

**Porosity: Level 0-6 mm.**
**Thin section**

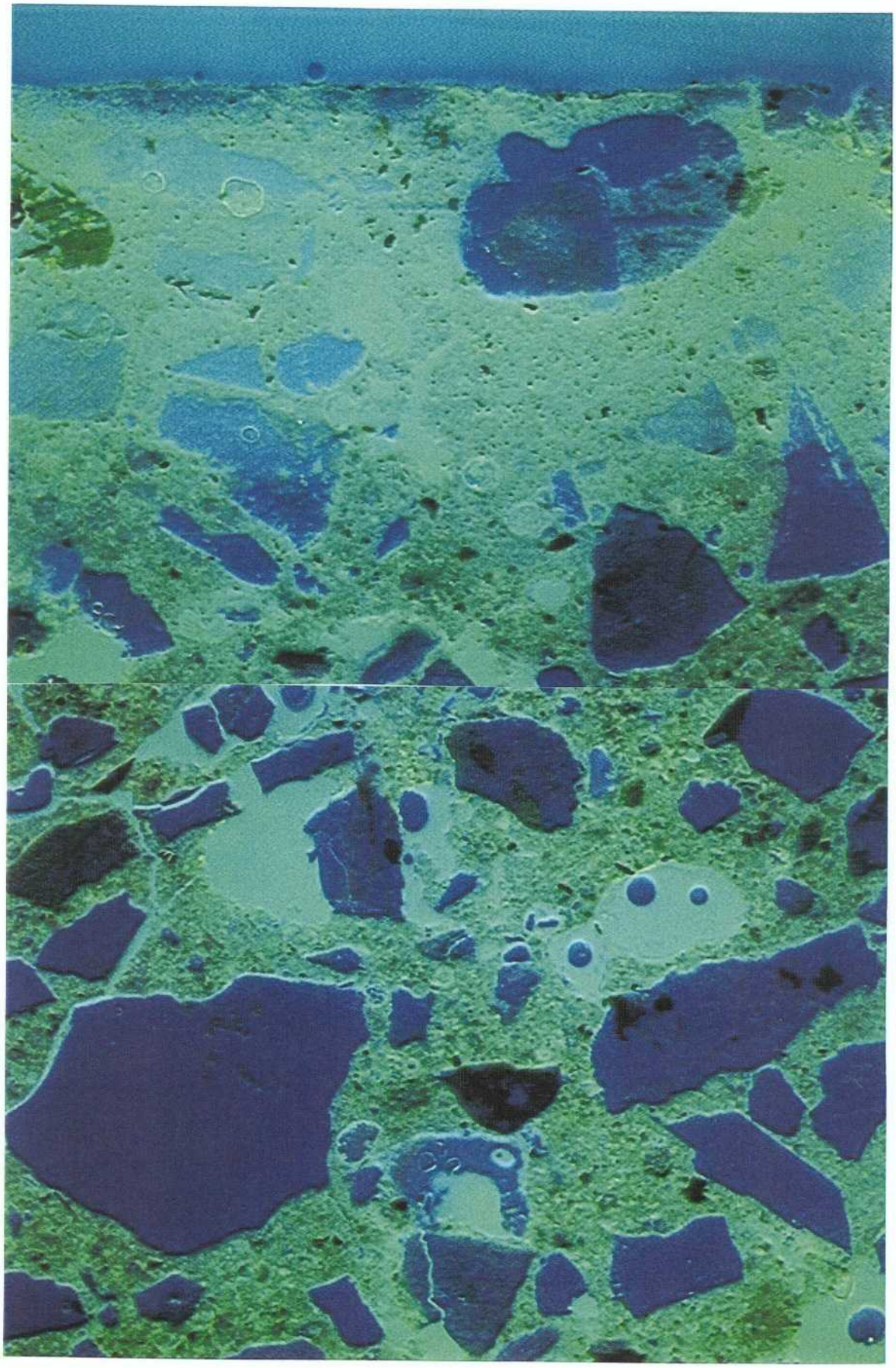


Fig 1.Porosity shown by fluorescent light under the microscope. Light areas indicate voids.

**Porosity: Level 6-10 mm.**

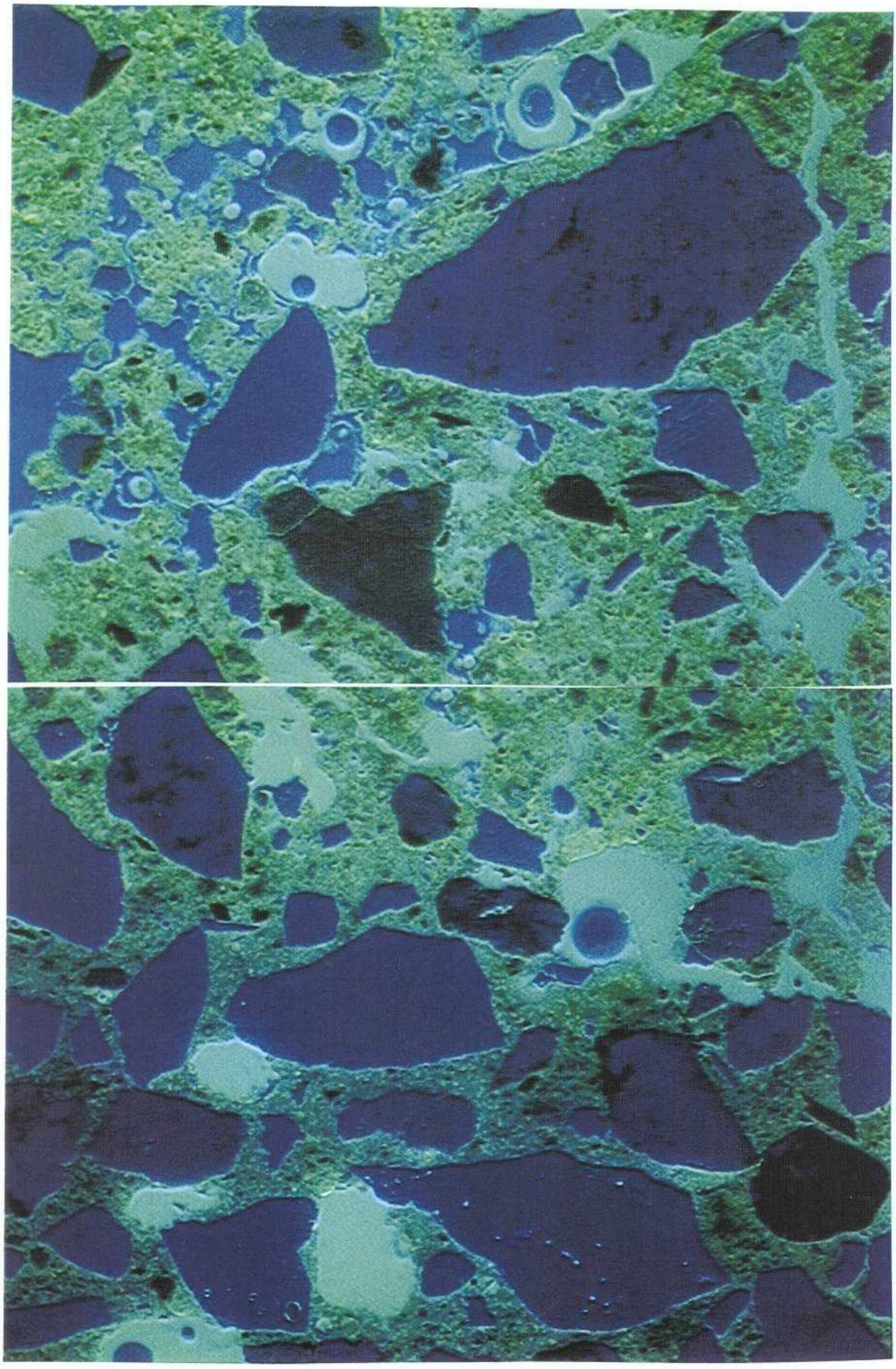


Fig 2. Irregular and "channel-like" voids indicate strong leaching. Note the sharp boundary between zones with coarse porosity and low porosity at about 9 mm.

**Porosity: Level 10-17 mm.**

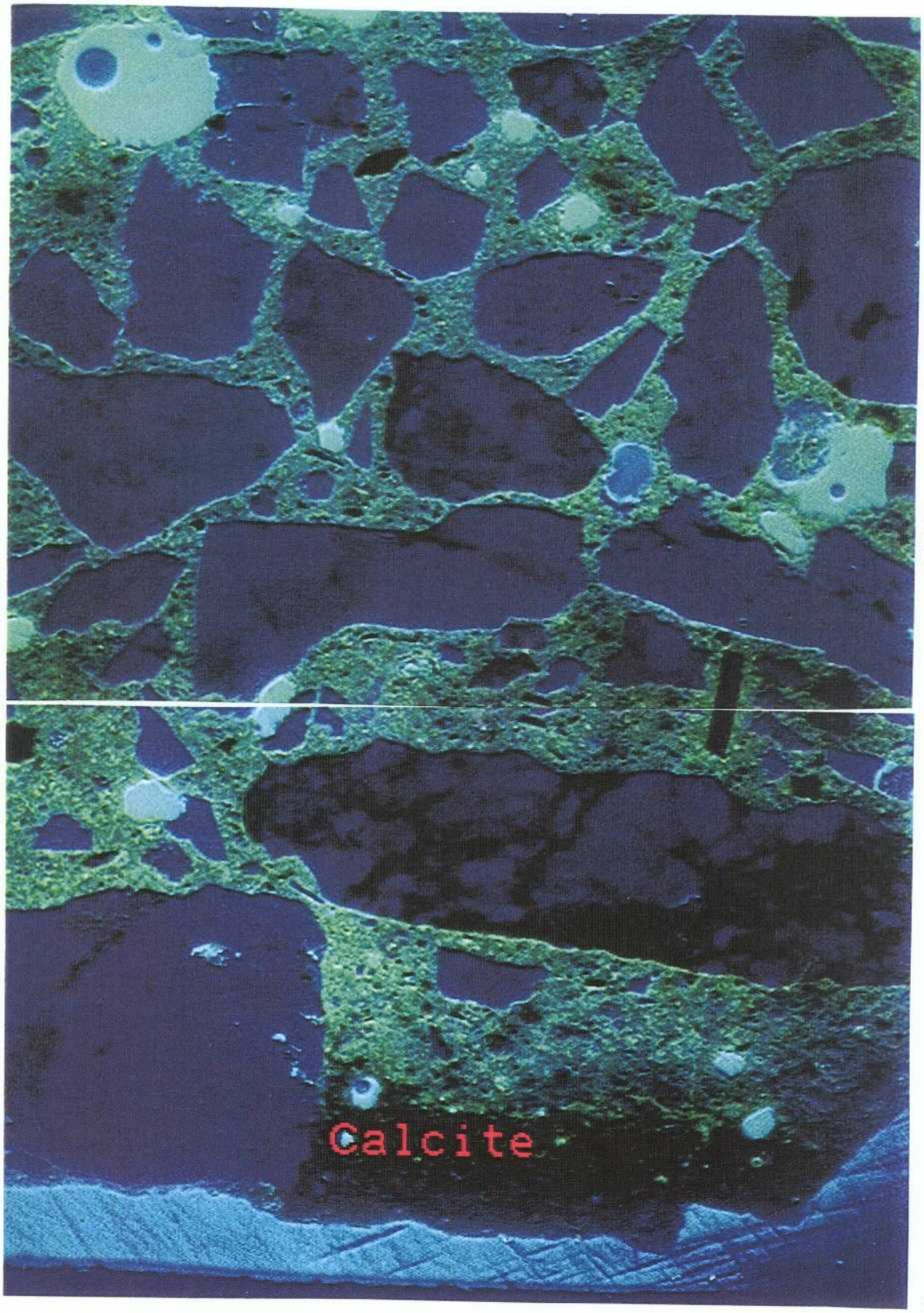


Fig 3. Zone with low porosity indicated by dark cement paste. Carbonation and calcite formation close to the steel confinement

SEM, Image Analysis

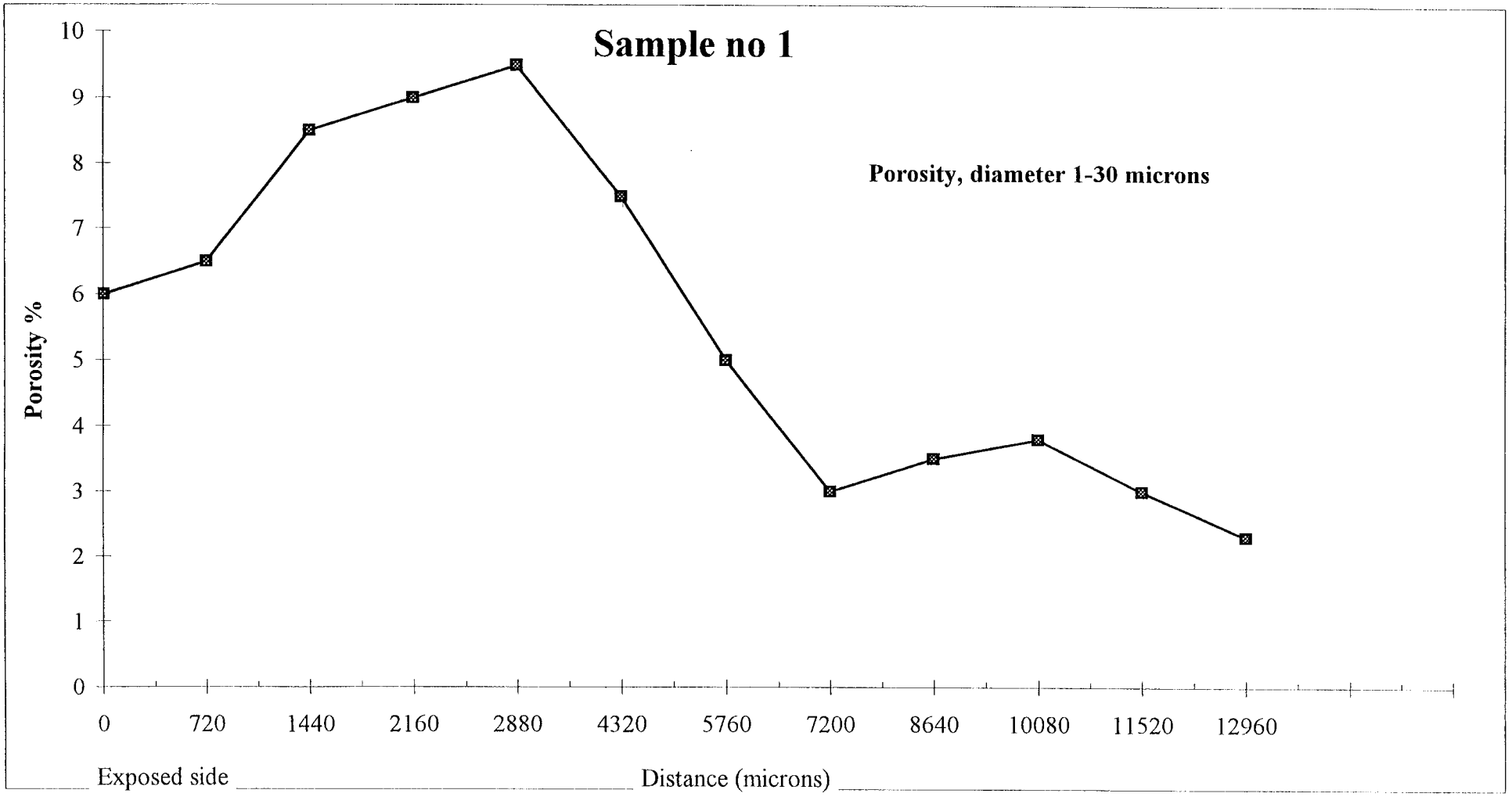

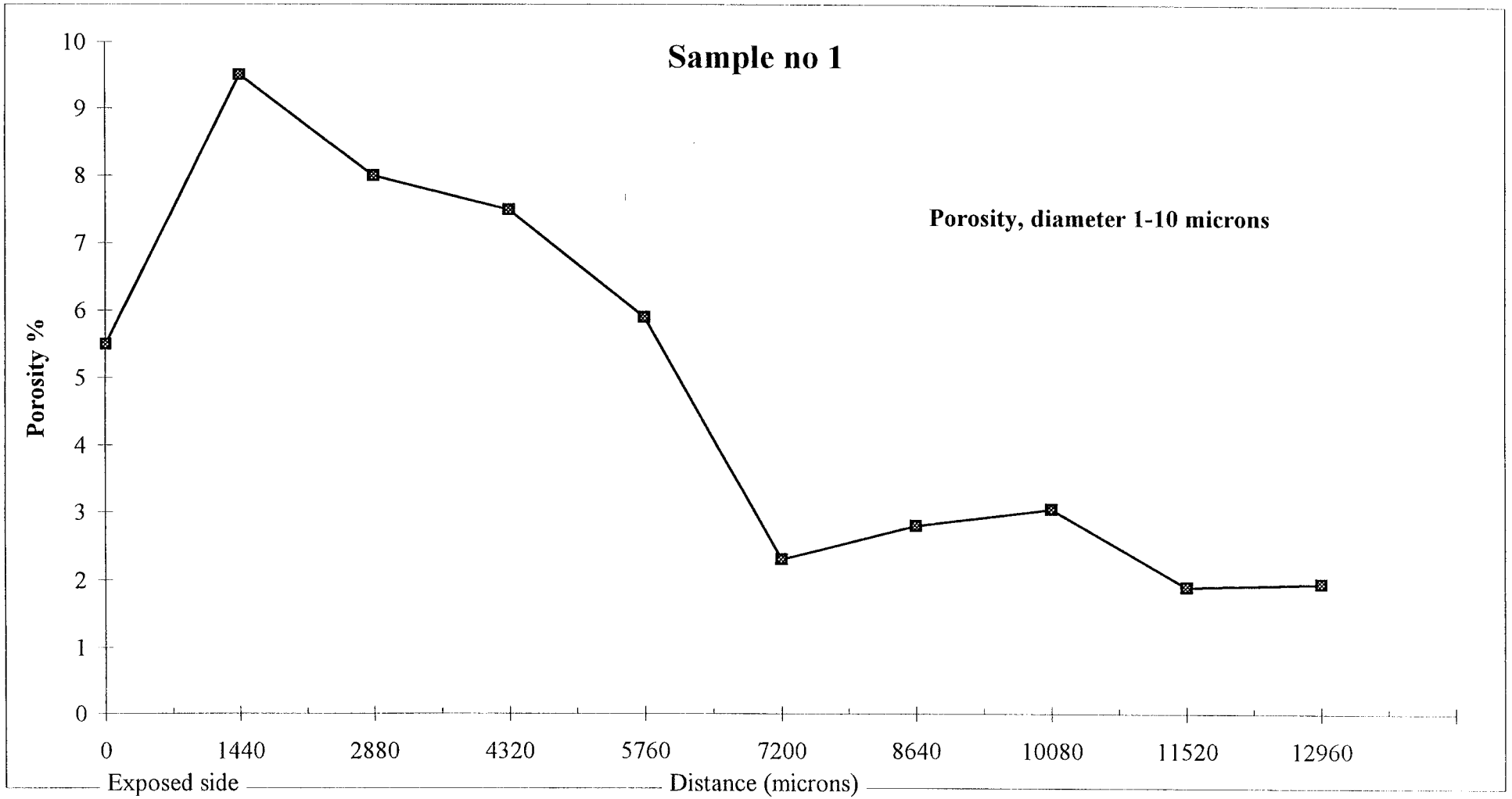
Sample no 1
Porosity, diameter 1-10 microns
Porosity %
10
9
8
7
6
5
4
3
2
1
0
0
1440
2880
4320
5760
7200
8640
10080
11520
12960
Exposed side
Distance (microns)

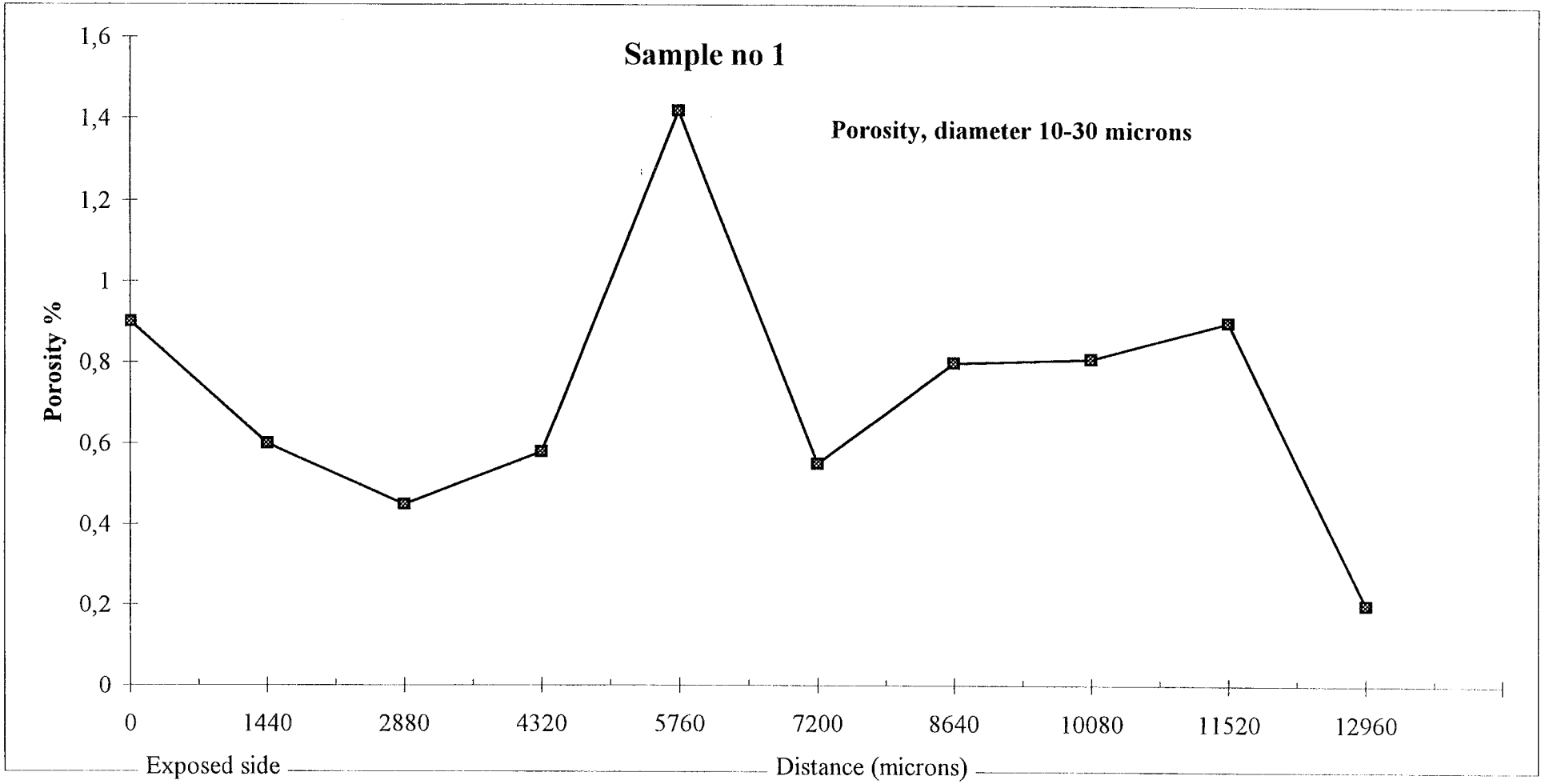
Sample no 1
Porosity, diameter 10-30 microns
Porosity %
1,6
1,4
1,2
1
0,8
0,6
0,4
0,2
0
0
1440
2880
4320
5760
7200
8640
10080
11520
12960
Exposed side
Distance (microns)

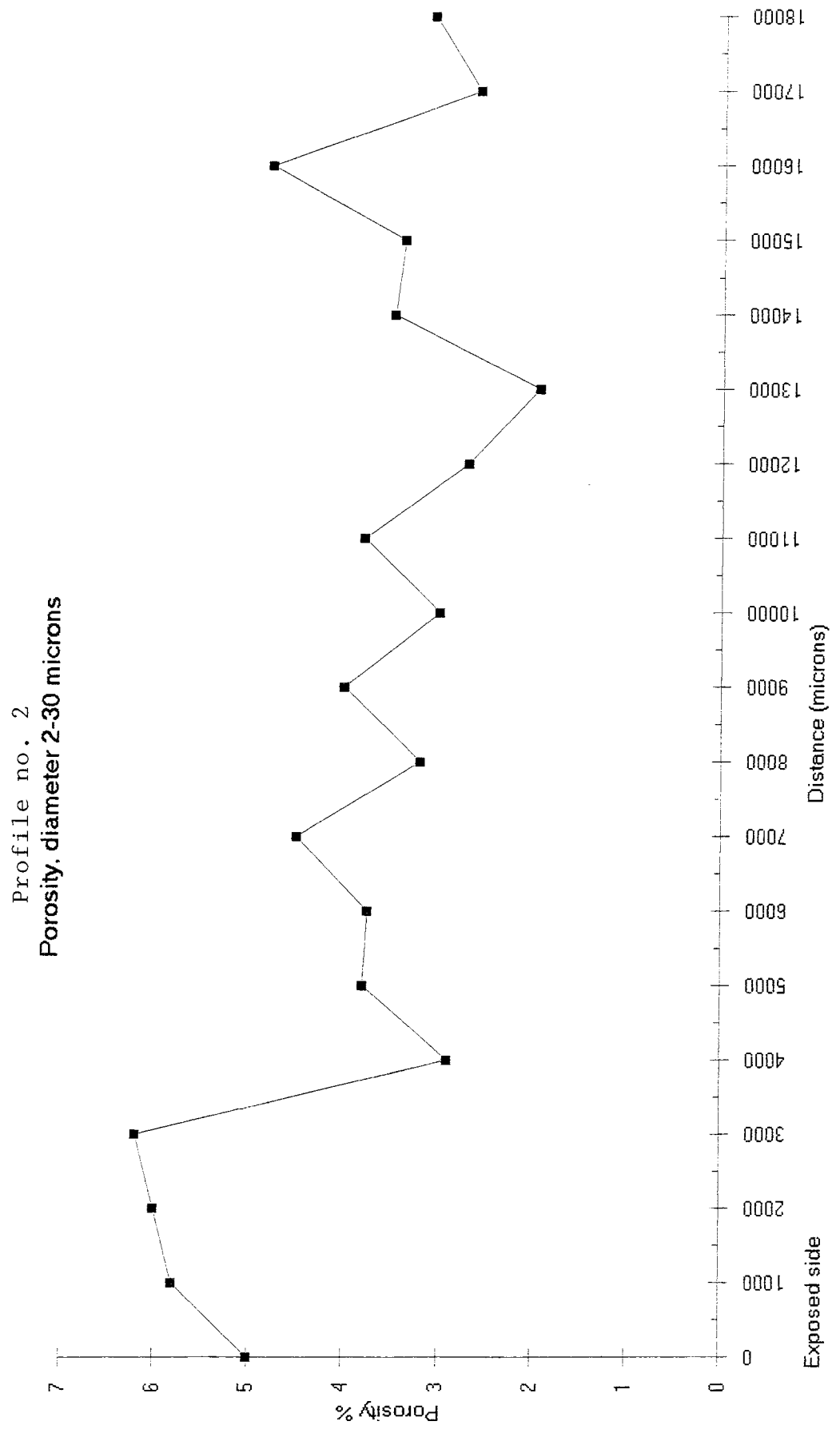
Profile no. 2
Porosity, diameter 2-30 microns
Porosity %
0
1
2
3
4
5
6
7
Distance (microns)
Exposed side
0
1000
2000
3000
4000
5000
6000
7000
8000
9000
10000
11000
12000
13000
14000
15000
16000
17000
18000

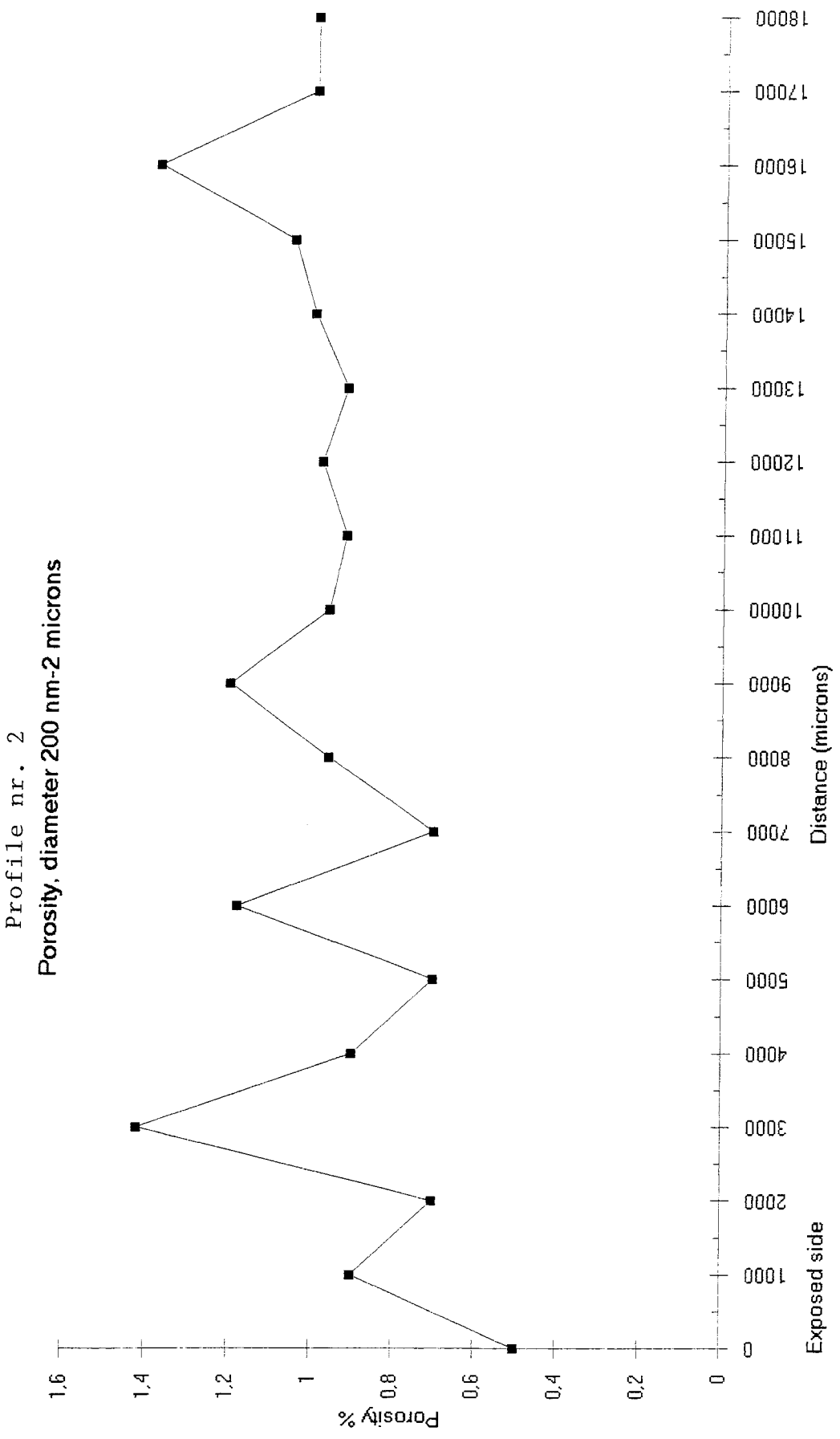
Profile nr. 2
Porosity, diameter 200 nm-2 microns
Porosity %
0
0,2
0,4
0,6
0,8
1
1,2
1,4
1,6
Distance (microns)
Exposed side
0
1000
2000
3000
4000
5000
6000
7000
8000
9000
10000
11000
12000
13000
14000
15000
16000
17000
18000

# Element distribution

## Sample number 1

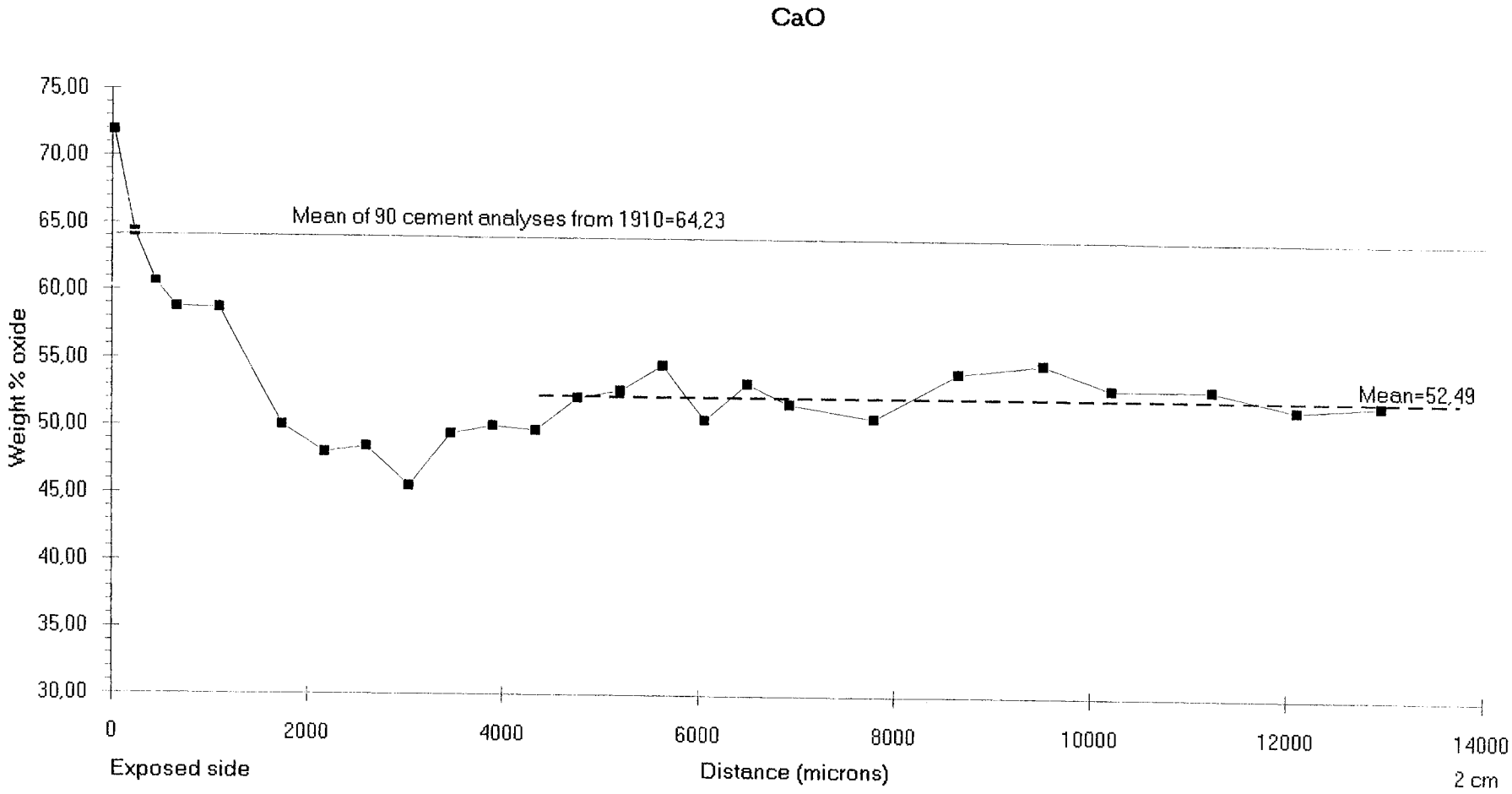
CaO
75,00
70,00
65,00
60,00
55,00
50,00
45,00
40,00
35,00
30,00
Weight % oxide
Mean of 90 cement analyses from 1910=64,23
Mean=52,49
0
2000
4000
6000
8000
10000
12000
14000
Exposed side
Distance (microns)
2 cm

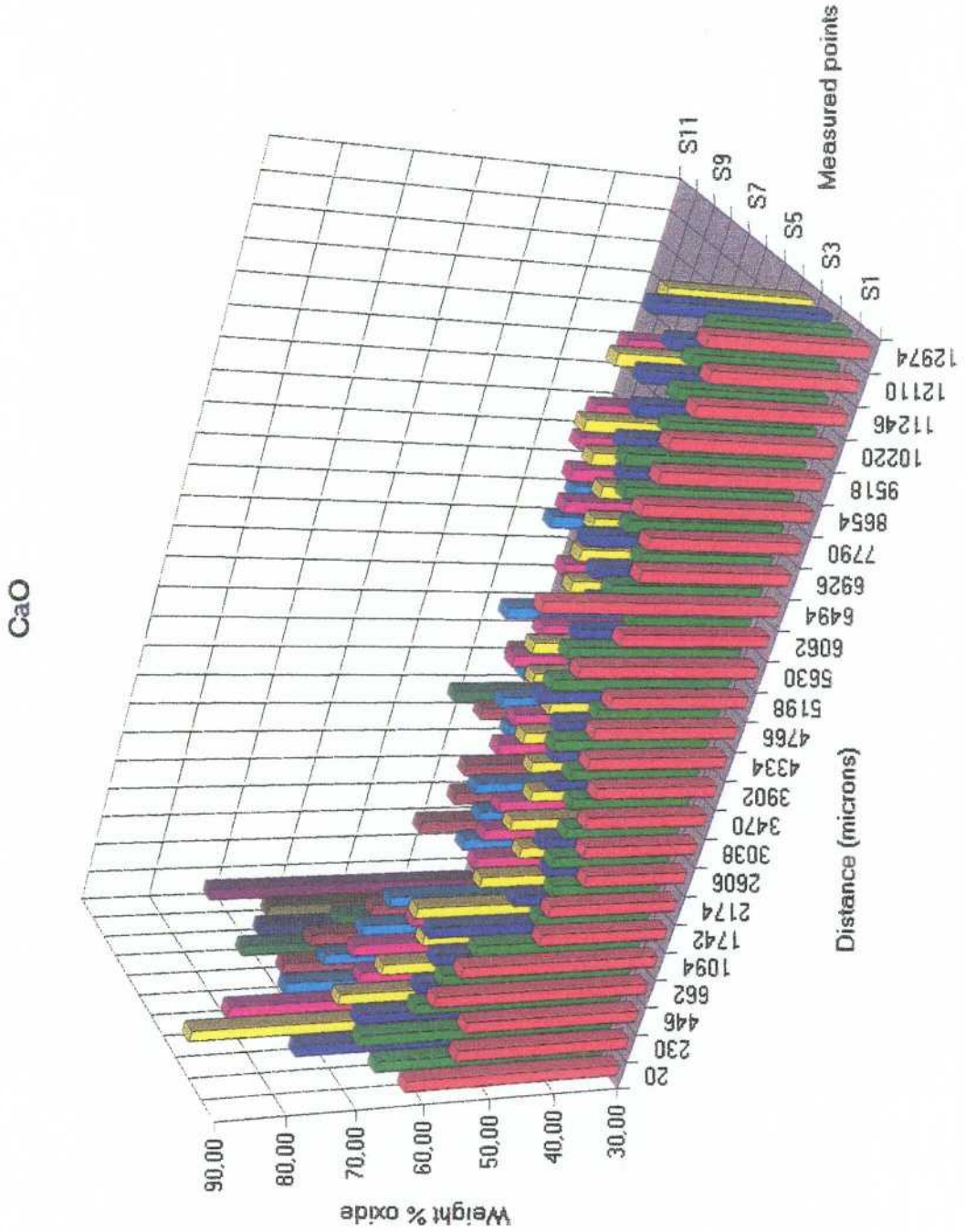
CaO
Weight % oxide
90,00
80,00
70,00
60,00
50,00
40,00
30,00
Distance (microns)
20
230
446
662
1094
1742
2174
2606
3038
3470
3902
4334
4766
5198
5630
6062
6494
6926
7790
8654
9518
10220
11246
12110
12974
Measured points
S1
S3
S5
S7
S9
S11

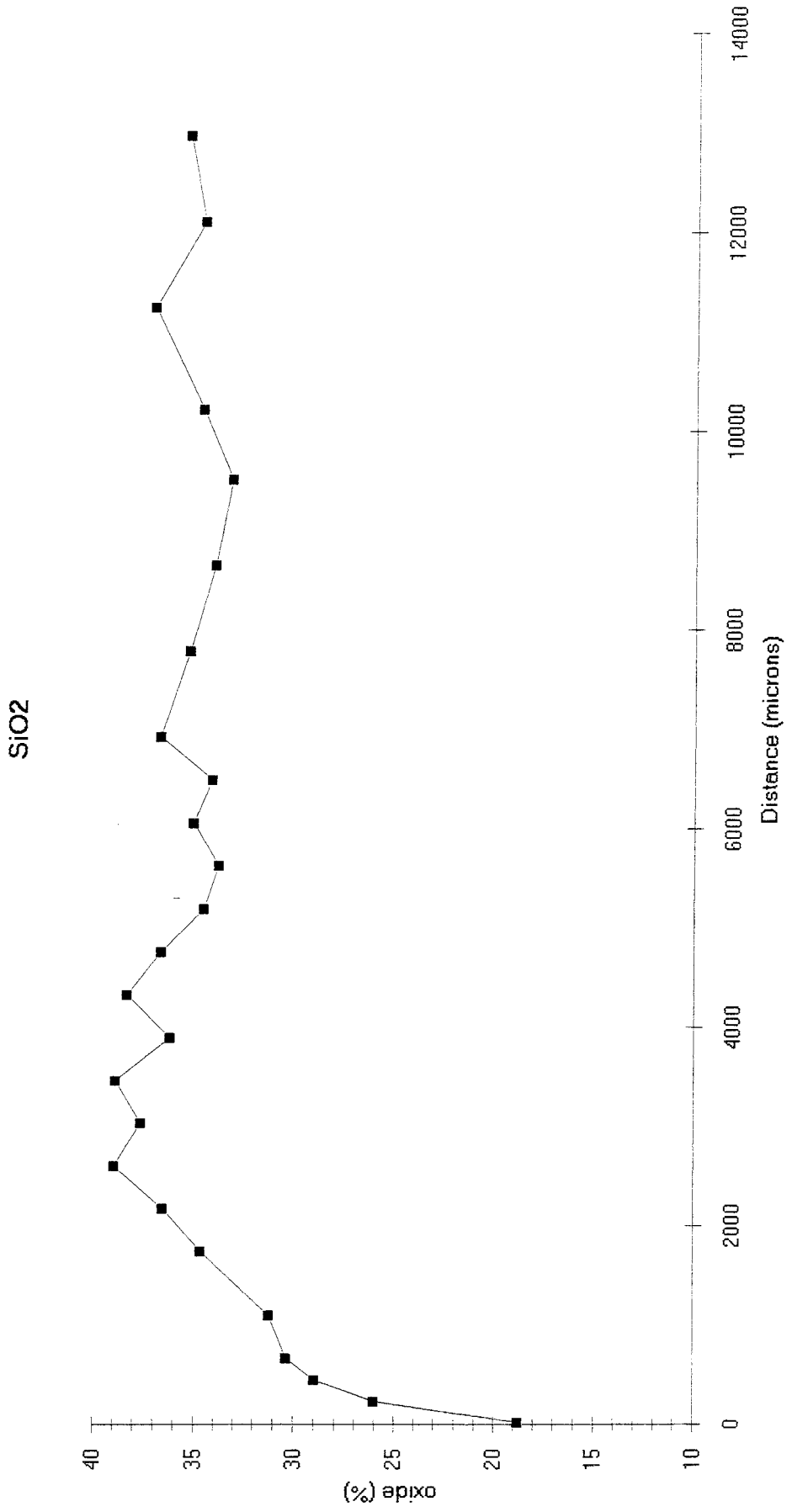
SiO2
oxide (%)
40
35
30
25
20
15
10
0
2000
4000
6000
8000
10000
12000
14000
Distance (microns)

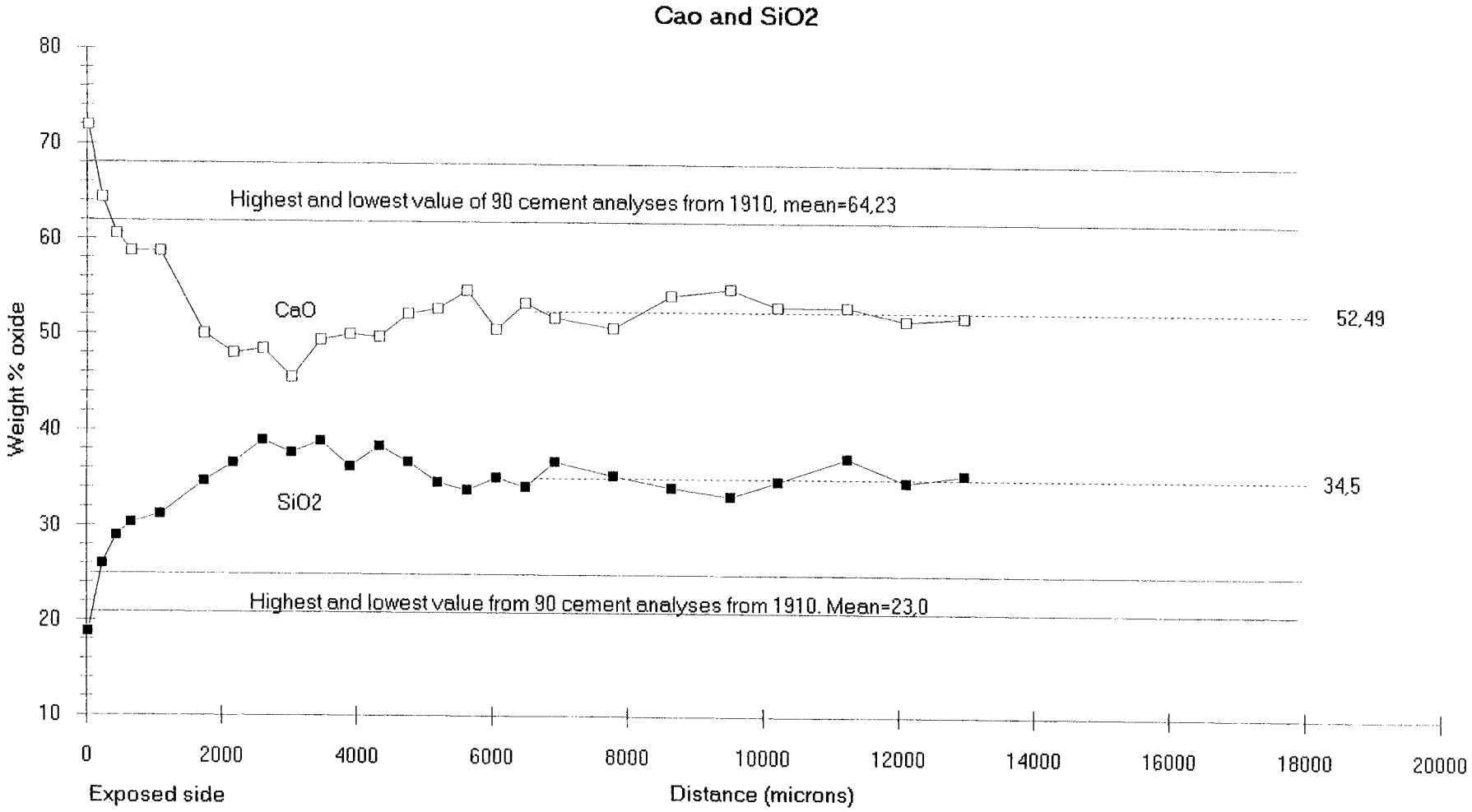
Cao and SiO2
Weight % oxide
80
70
60
50
40
30
20
10
Highest and lowest value of 90 cement analyses from 1910, mean=64,23
CaO
52,49
SiO2
34,5
Highest and lowest value from 90 cement analyses from 1910. Mean=23,0
0
2000
4000
6000
8000
10000
12000
14000
16000
18000
20000
Exposed side
Distance (microns)

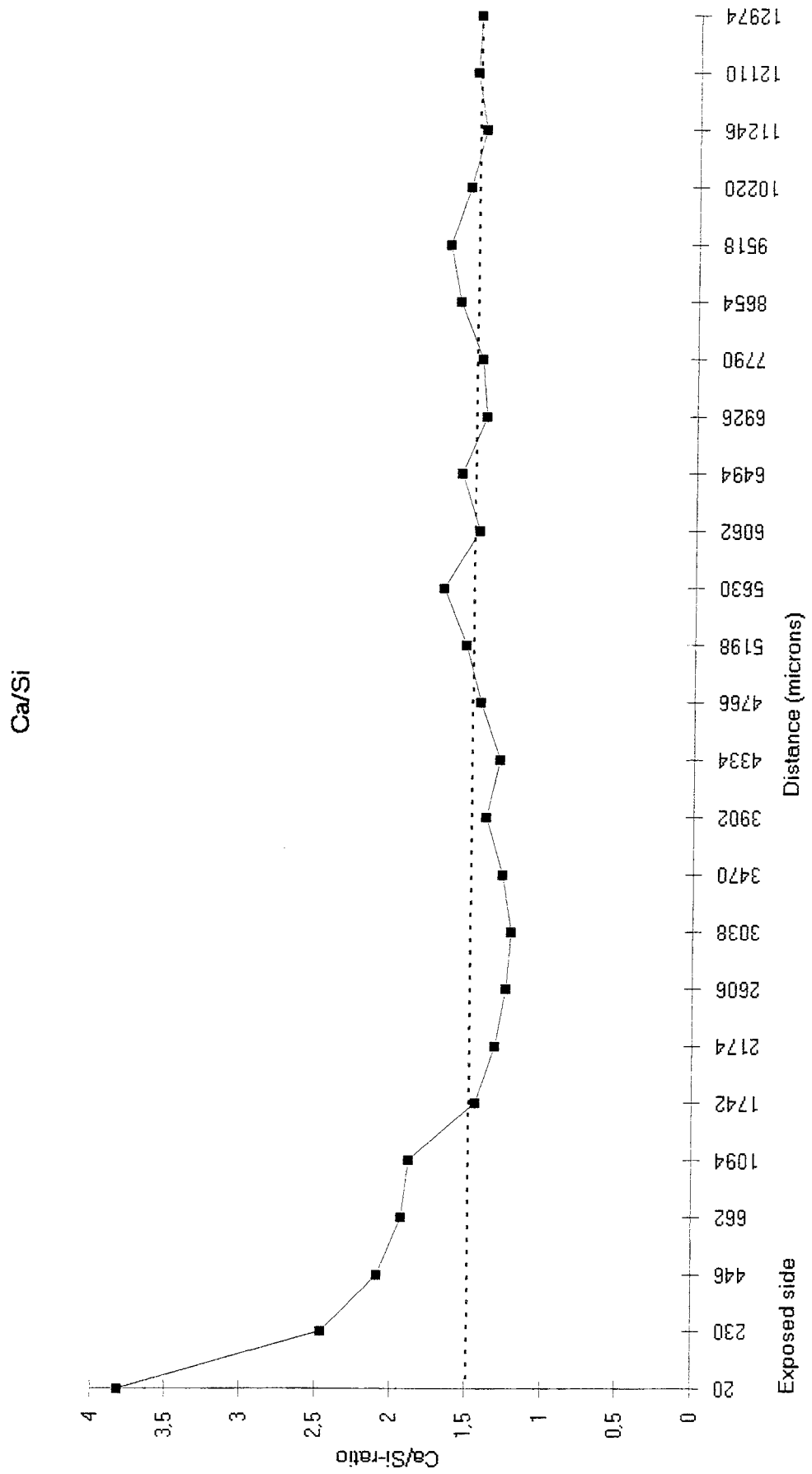
Ca/Si
Ca/Si-ratio
0
0,5
1
1,5
2
2,5
3
3,5
4
Distance (microns)
Exposed side
20
230
446
662
1094
1742
2174
2606
3038
3470
3902
4334
4766
5198
5630
6062
6494
6926
7790
8654
9518
10220
11246
12110
12974

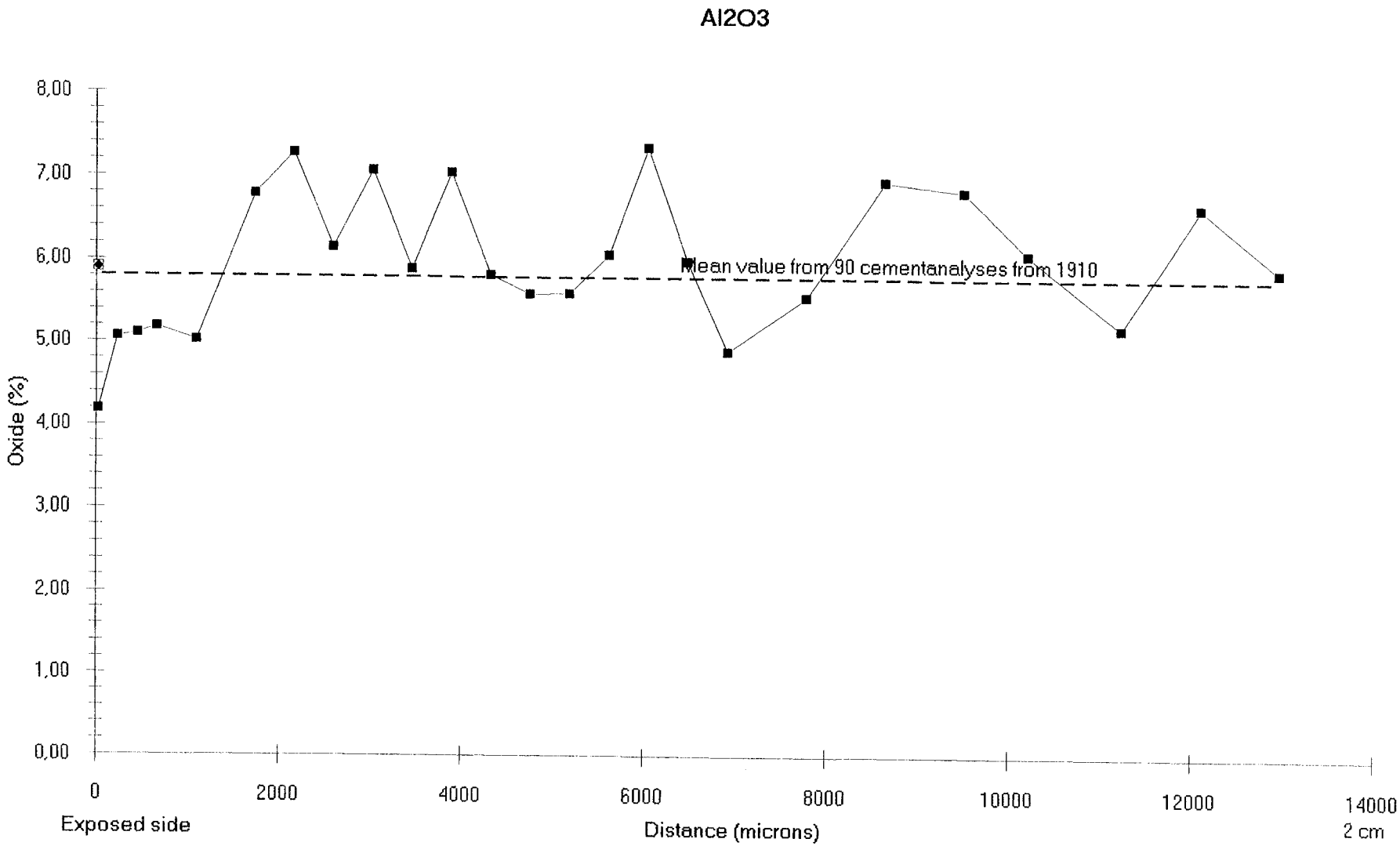
Al2O3
8,00
7,00
6,00
5,00
4,00
3,00
2,00
1,00
0,00
Oxide (%)
Mean value from 90 cementanalyses from 1910
0
2000
4000
6000
8000
10000
12000
14000
Exposed side
Distance (microns)
2 cm

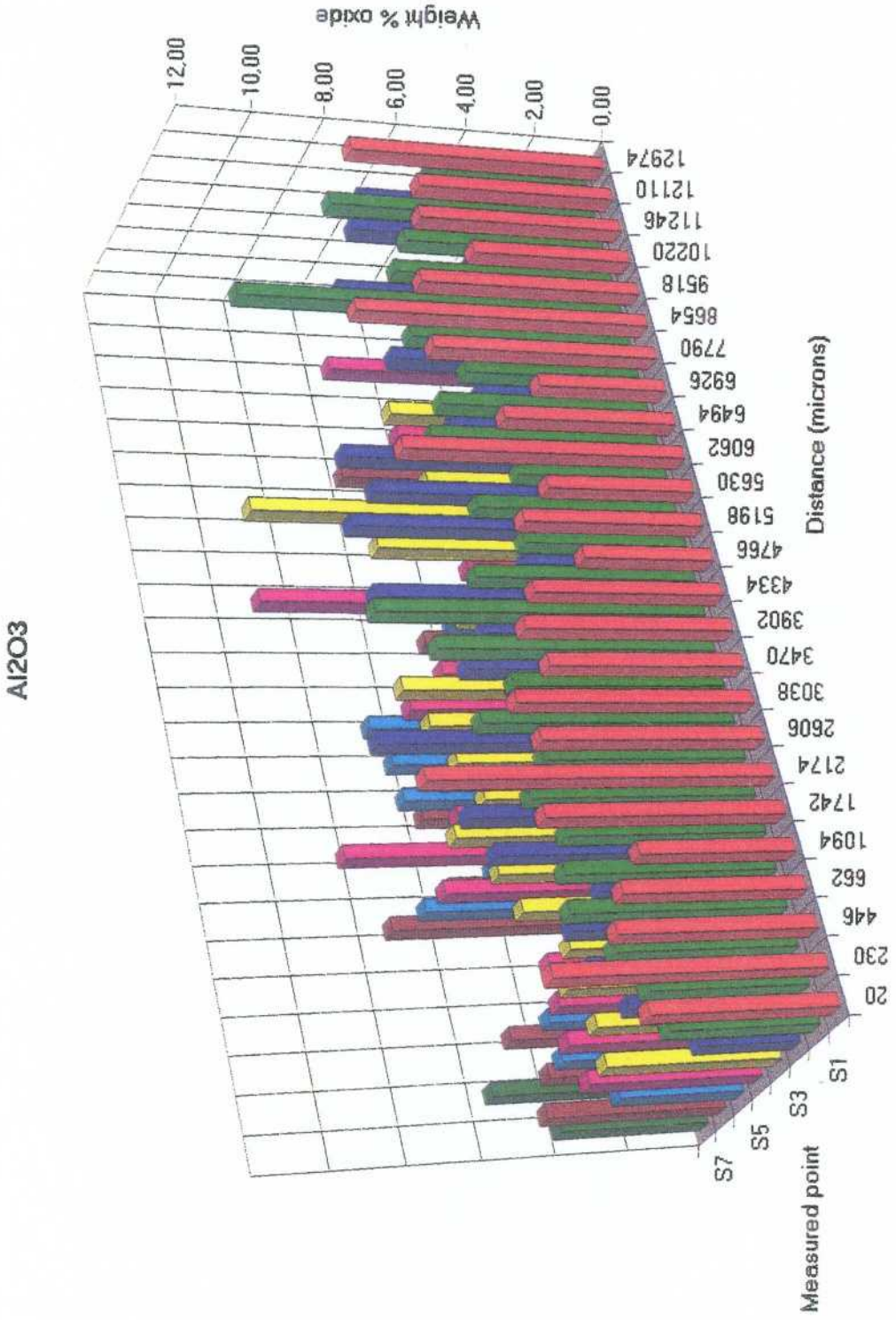
Al2O3
Weight % oxide
12,00
10,00
8,00
6,00
4,00
2,00
0,00
Distance (microns)
12974
12110
11246
10220
9518
8654
7790
6926
6494
6062
5630
5198
4766
4334
3902
3470
3038
2606
2174
1742
1094
662
446
230
20
Measured point
S1
S3
S5
S7

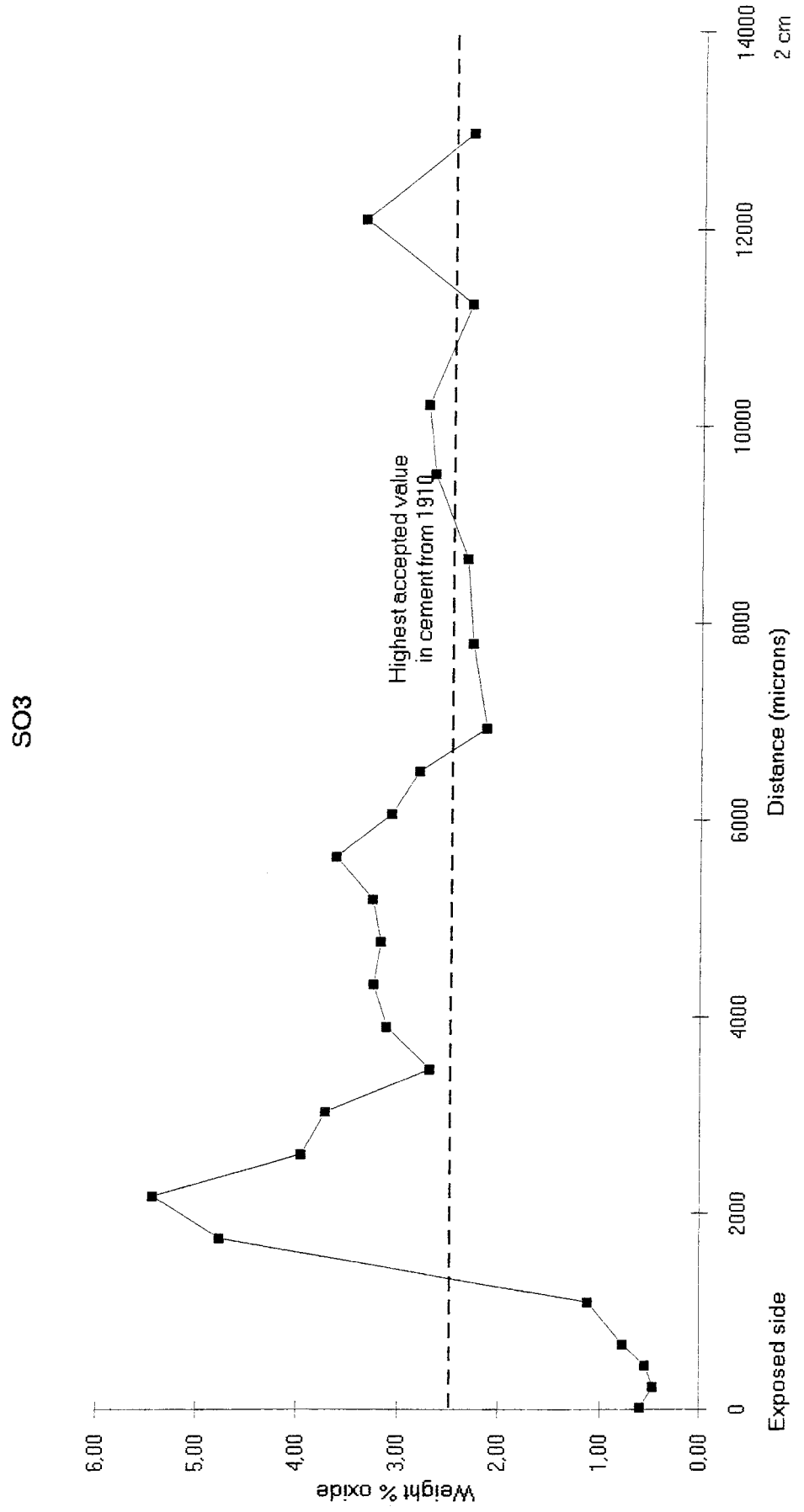
SO3
Highest accepted value
in cement from 1910
Weight % oxide
6,00
5,00
4,00
3,00
2,00
1,00
0,00
0
2000
4000
6000
8000
10000
12000
14000
Distance (microns)
Exposed side
2 cm

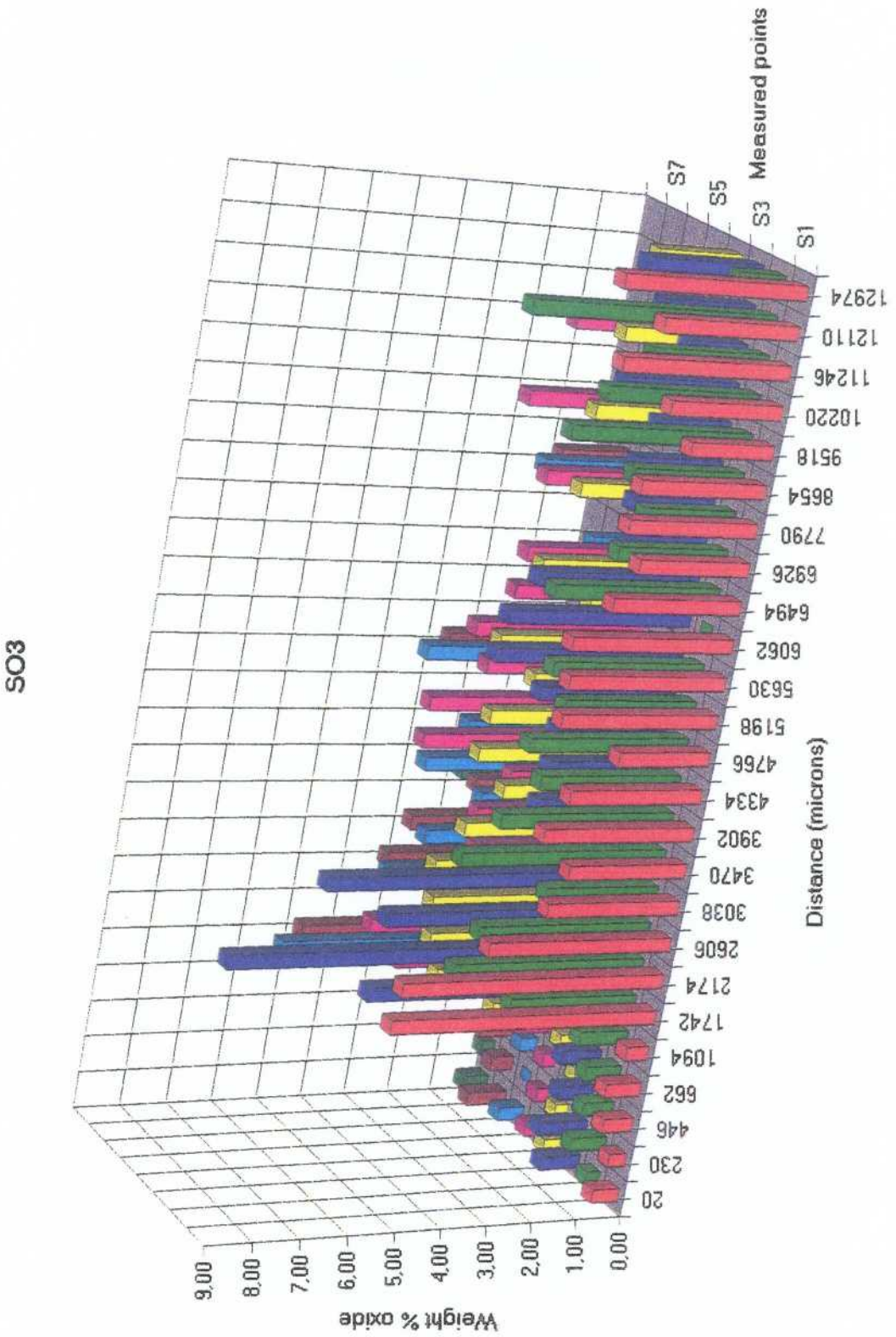
SO3
Measured points
S7
S5
S3
S1
Distance (microns)
12974
12110
11246
10220
9518
8654
7790
6926
6494
6062
5630
5198
4766
4334
3902
3470
3038
2606
2174
1742
1094
662
446
230
20
Weight % oxide
9,00
8,00
7,00
6,00
5,00
4,00
3,00
2,00
1,00
0,00

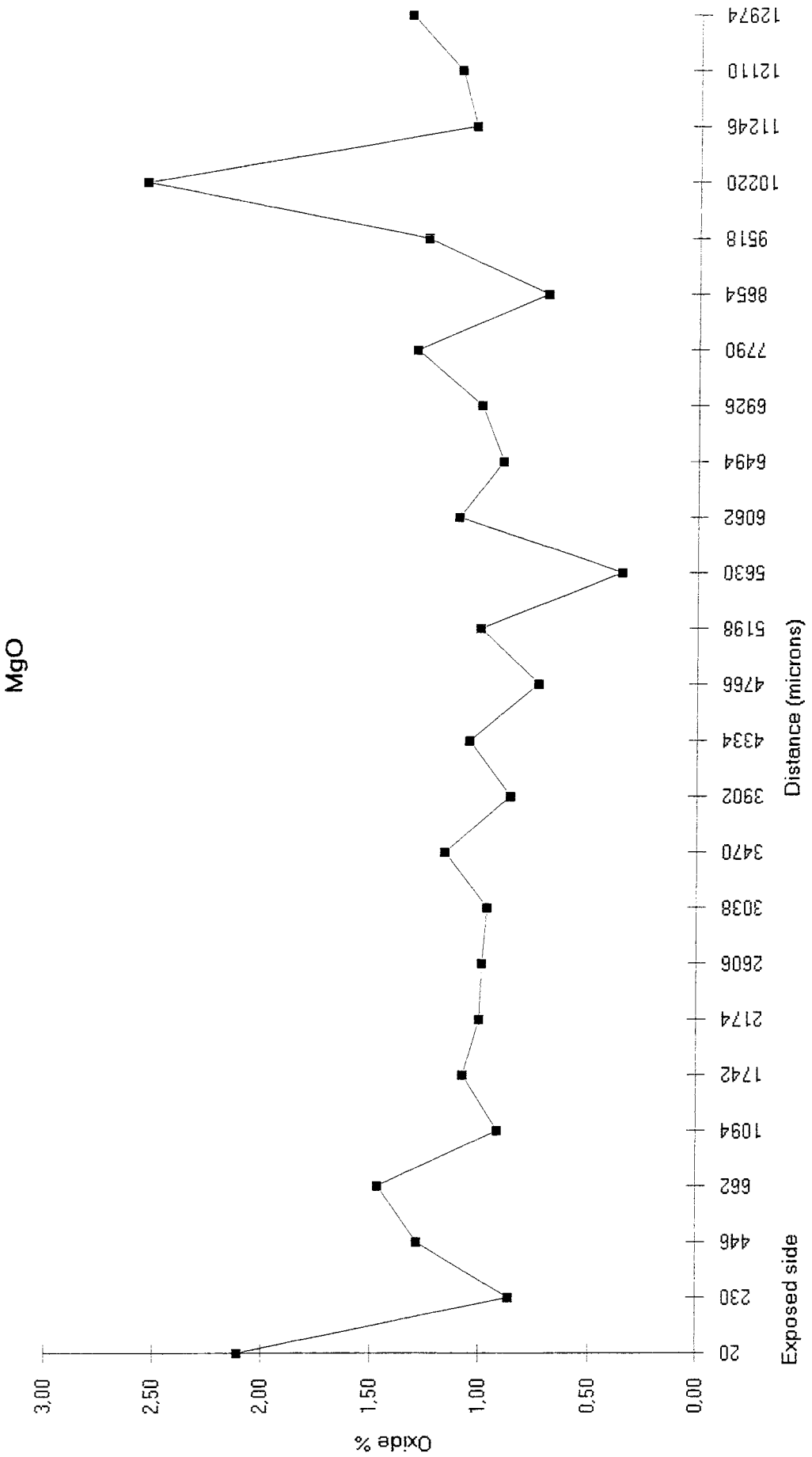
MgO
Oxide %
3,00
2,50
2,00
1,50
1,00
0,50
0,00
Distance (microns)
Exposed side
20
230
446
662
1094
1742
2174
2606
3038
3470
3902
4334
4766
5198
5630
6062
6494
6926
7790
8654
9518
10220
11246
12110
12974

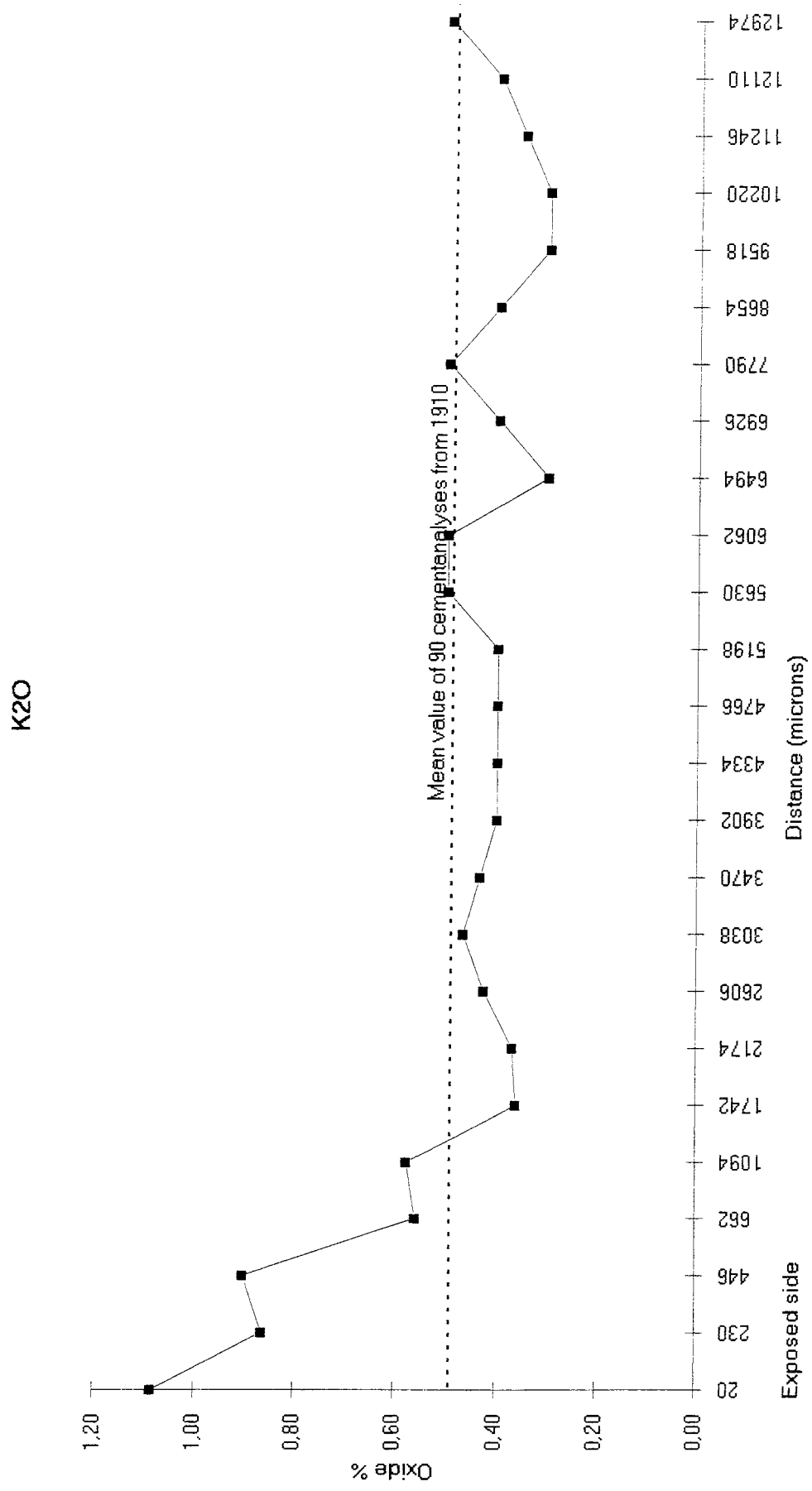
K2O
Mean value of 90 cementanalyses from 1910
Oxide %
1,20
1,00
0,80
0,60
0,40
0,20
0,00
Distance (microns)
Exposed side
20
230
446
662
1094
1742
2174
2606
3038
3470
3902
4334
4766
5198
5630
6062
6494
6926
7790
8654
9518
10220
11246
12110
12974

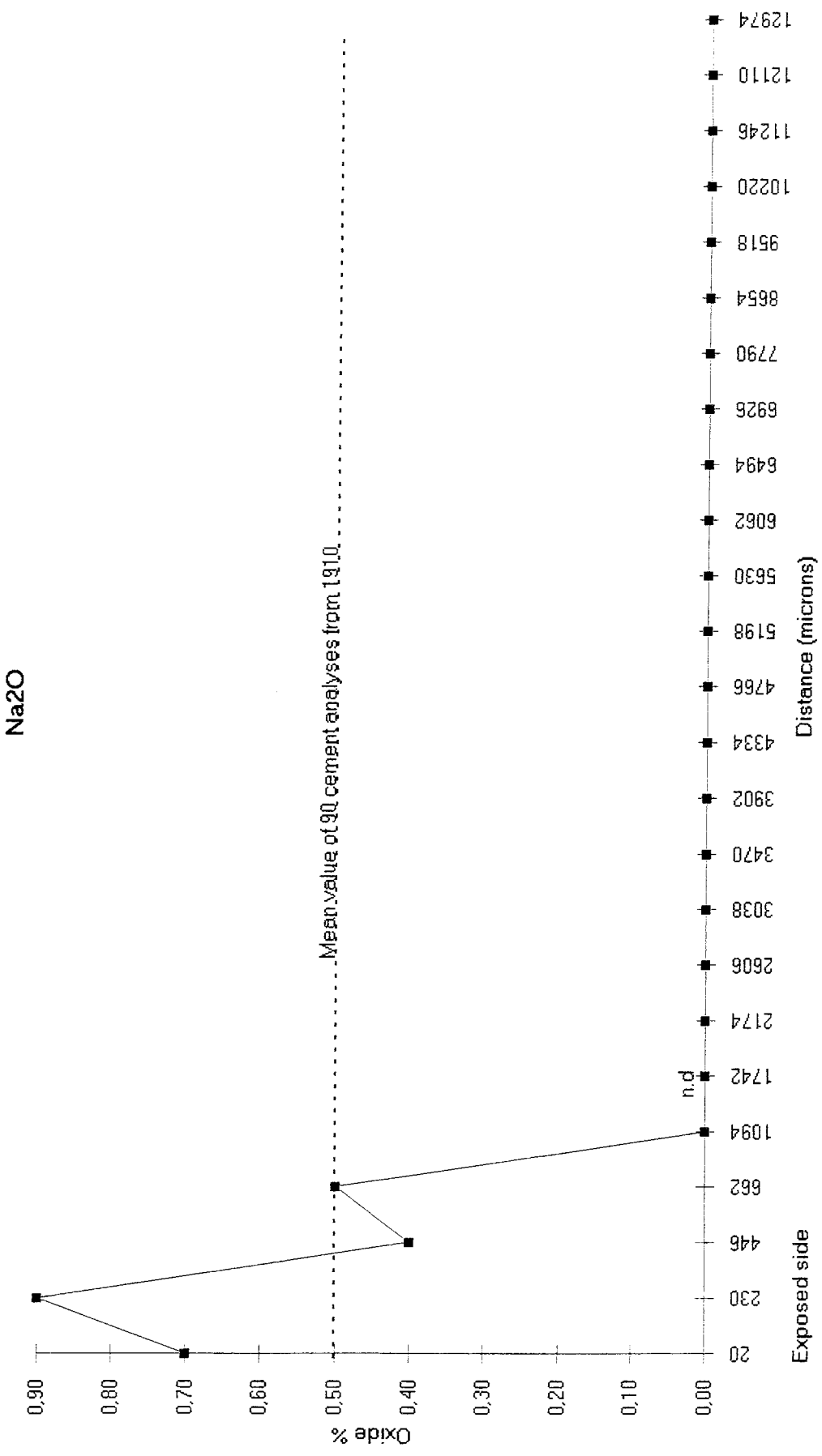
Na2O
Mean value of 90 cement analyses from 1910
Oxide %
0,90
0,80
0,70
0,60
0,50
0,40
0,30
0,20
0,10
0,00
Distance (microns)
Exposed side
20
230
446
662
1094
n.d
1742
2174
2606
3038
3470
3902
4334
4766
5198
5630
6062
6494
6926
7790
8654
9518
10220
11246
12110
12974

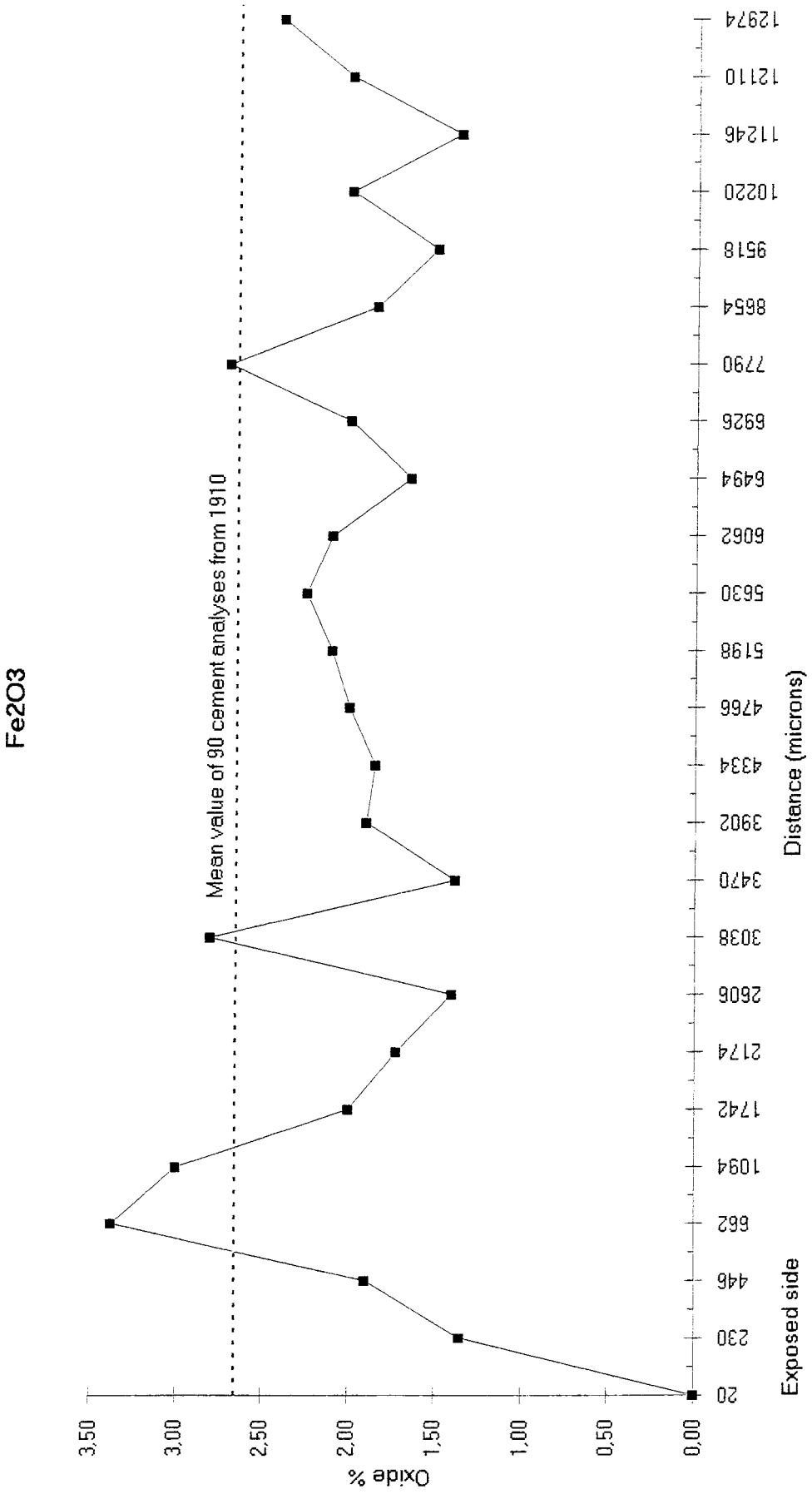
Fe2O3
Mean value of 90 cement analyses from 1910
Oxide %
3,50
3,00
2,50
2,00
1,50
1,00
0,50
0,00
Distance (microns)
Exposed side
20
230
446
662
1094
1742
2174
2606
3038
3470
3902
4334
4766
5198
5630
6062
6494
6926
7790
8654
9518
10220
11246
12110
12974

# Element distribution

## Sample number 2

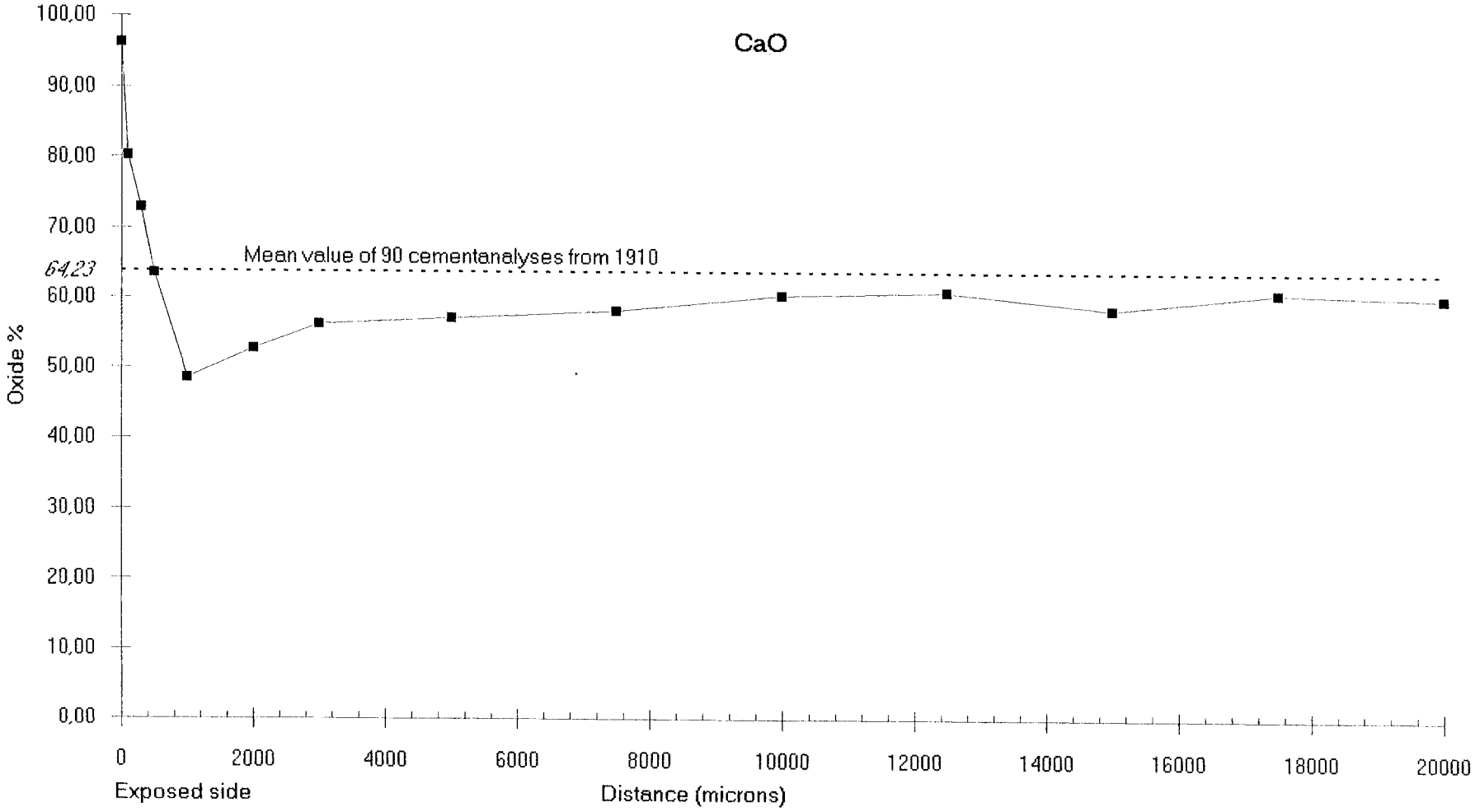
CaO
100,00
90,00
80,00
70,00
64,23
60,00
50,00
40,00
30,00
20,00
10,00
0,00
Oxide %
Mean value of 90 cementanalyses from 1910
0
2000
4000
6000
8000
10000
12000
14000
16000
18000
20000
Exposed side
Distance (microns)

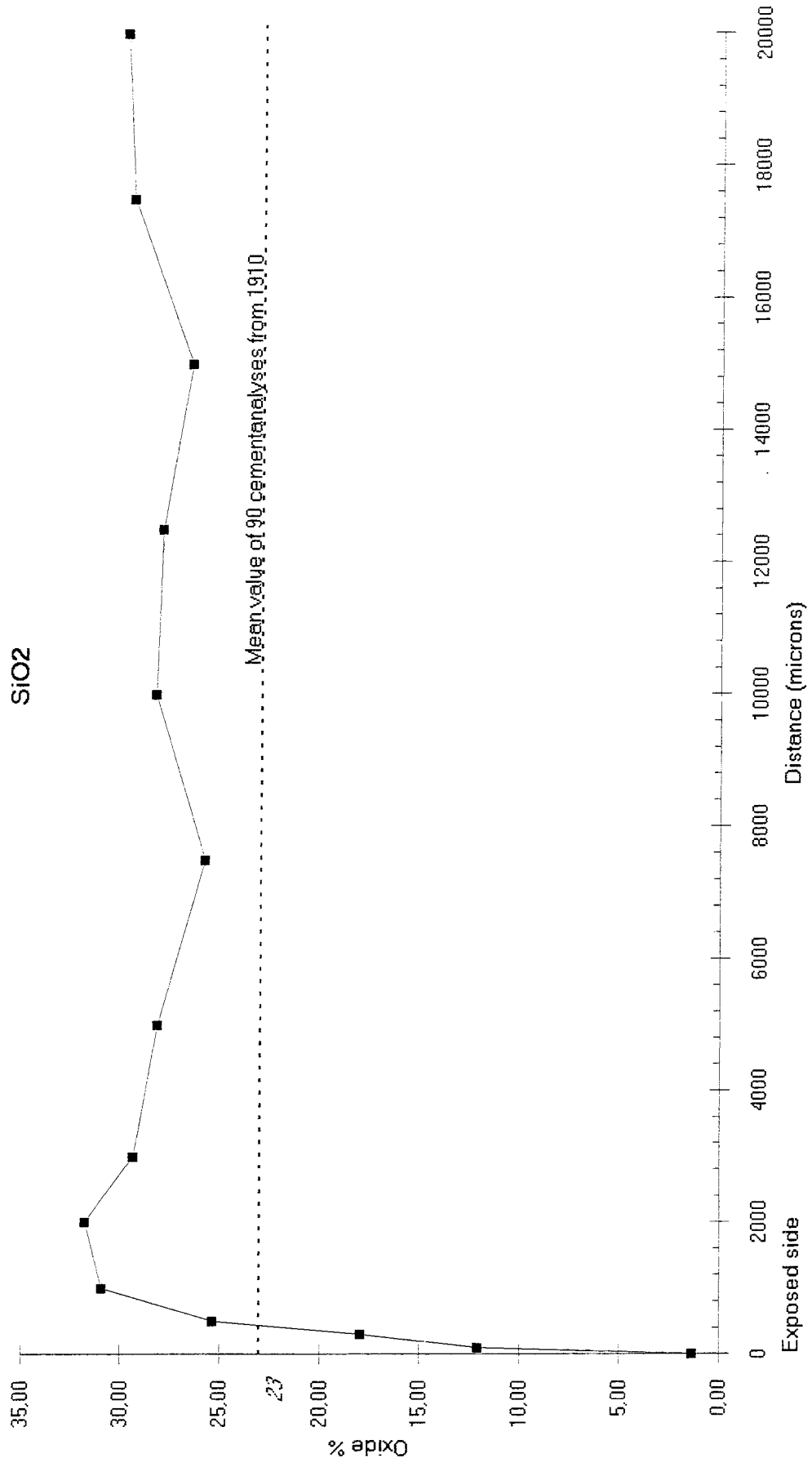
SiO2
Mean value of 90 cementanalyses from 1910
23
Oxide %
35,00
30,00
25,00
20,00
15,00
10,00
5,00
0,00
Exposed side
0
2000
4000
6000
8000
10000
12000
14000
16000
18000
20000
Distance (microns)

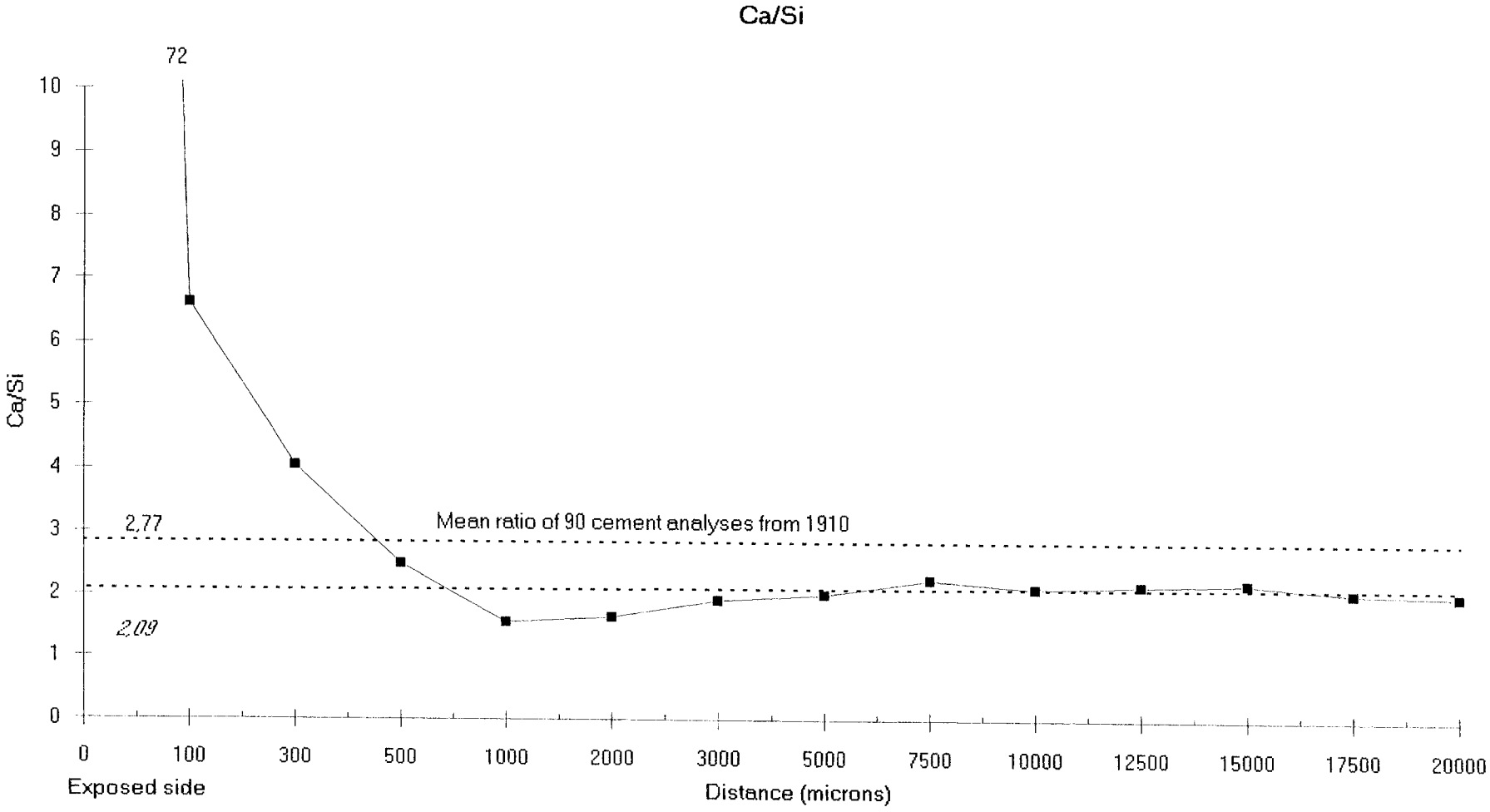
Ca/Si
72
10
9
8
7
6
5
4
3
2
1
0
Ca/Si
2.77
Mean ratio of 90 cement analyses from 1910
2.09
0
100
300
500
1000
2000
3000
5000
7500
10000
12500
15000
17500
20000
Exposed side
Distance (microns)

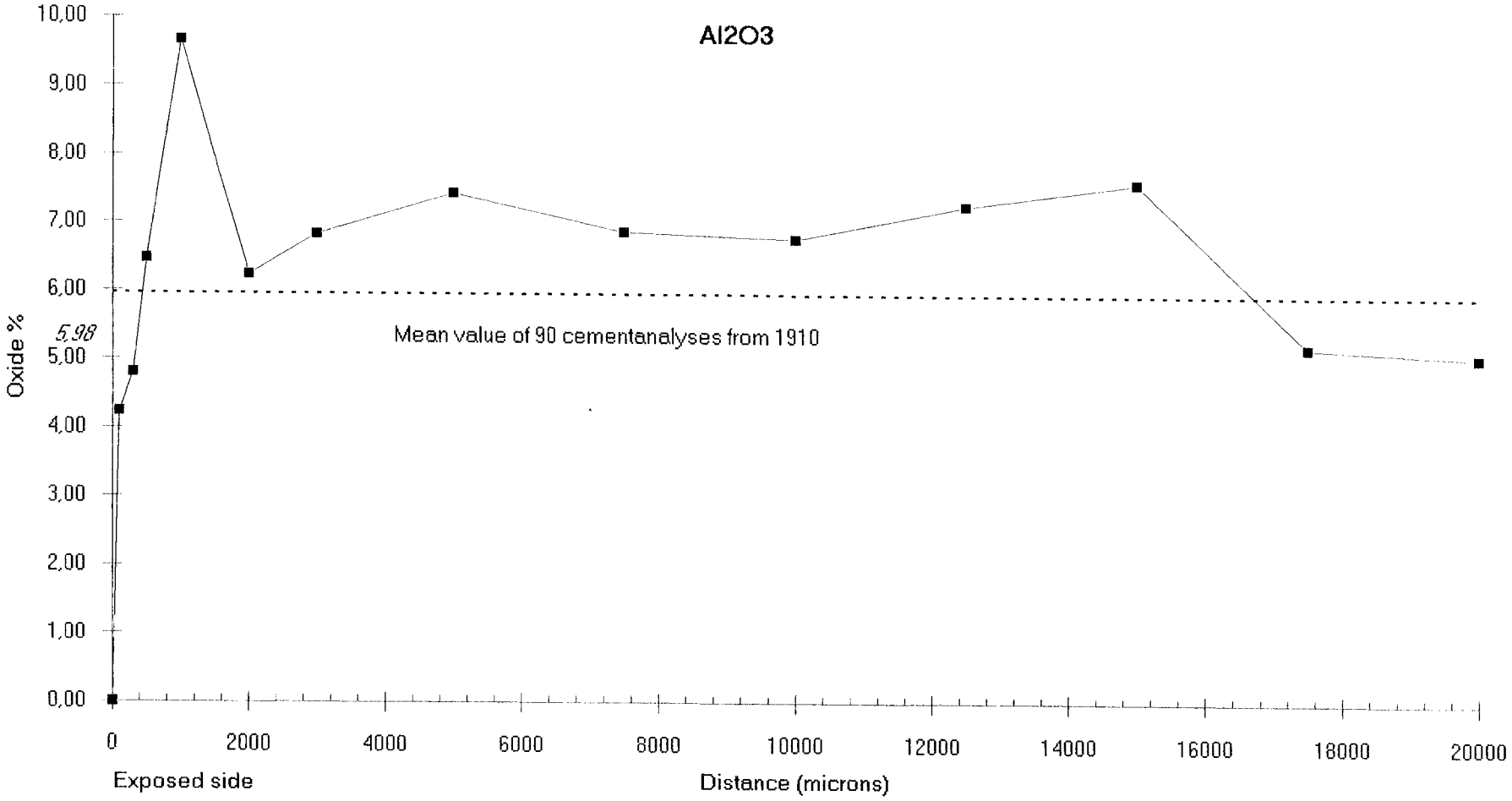
Al2O3
Oxide %
10,00
9,00
8,00
7,00
6,00
5,98
5,00
4,00
3,00
2,00
1,00
0,00
Mean value of 90 cementanalyses from 1910
0
2000
4000
6000
8000
10000
12000
14000
16000
18000
20000
Exposed side
Distance (microns)

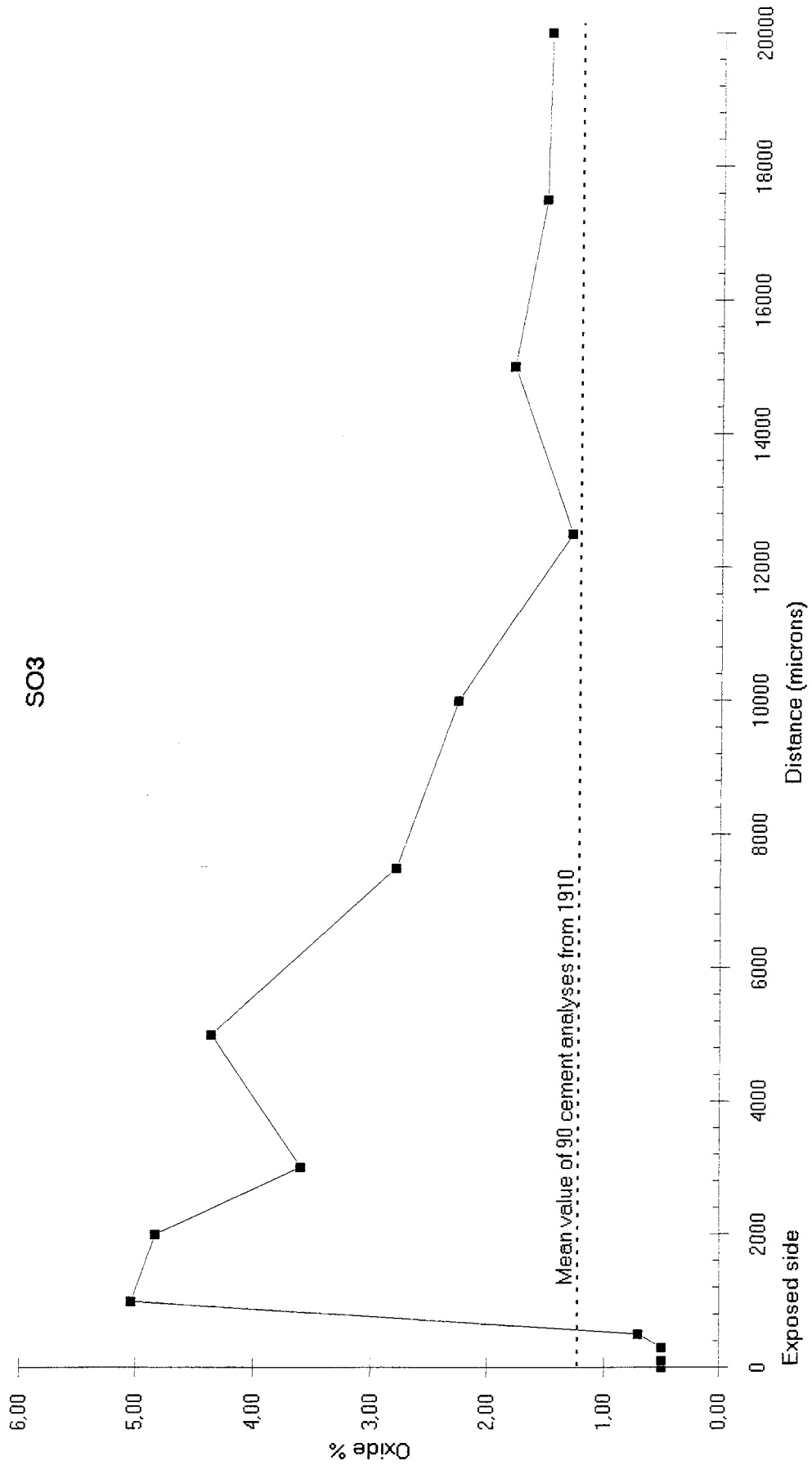
SO3
Oxide %
6,00
5,00
4,00
3,00
2,00
1,00
0,00
Mean value of 90 cement analyses from 1910
0
2000
4000
6000
8000
10000
12000
14000
16000
18000
20000
Exposed side
Distance (microns)

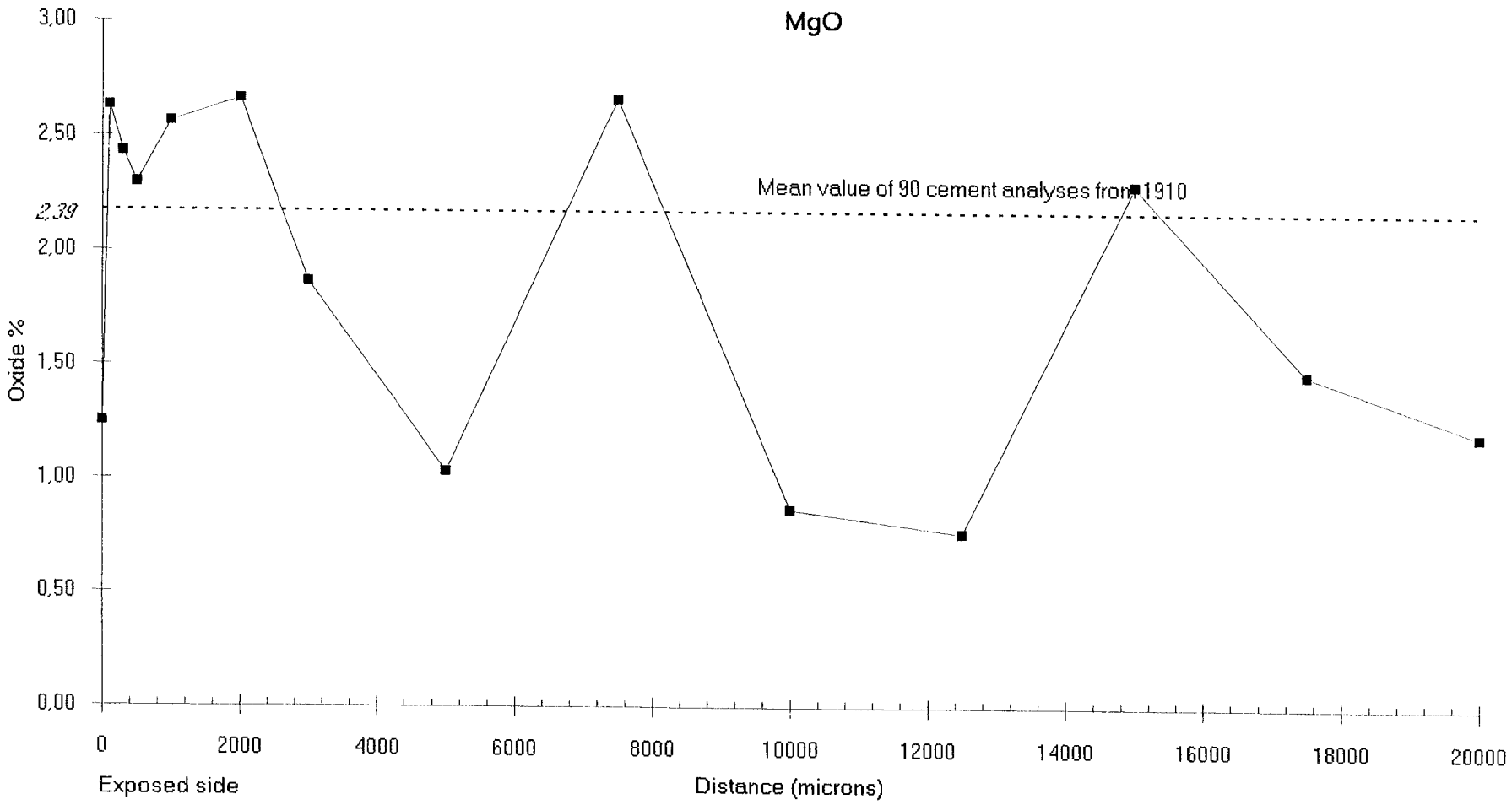
MgO
3,00
2,50
2,39
2,00
1,50
1,00
0,50
0,00
Oxide %
Mean value of 90 cement analyses from 1910
0
2000
4000
6000
8000
10000
12000
14000
16000
18000
20000
Exposed side
Distance (microns)

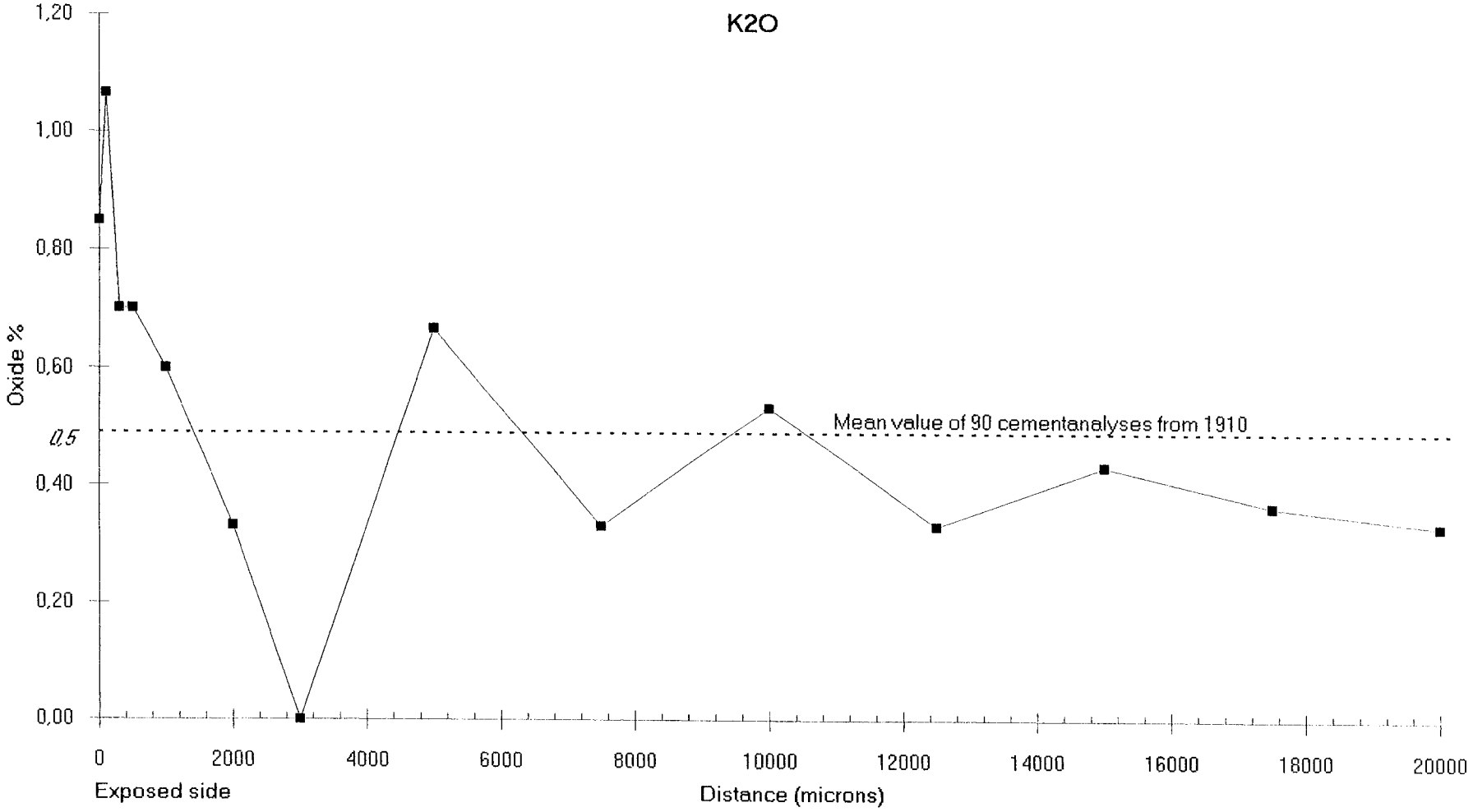
K2O
1,20
1,00
0,80
0,60
0,5
0,40
0,20
0,00
Oxide %
Mean value of 90 cementanalyses from 1910
0
2000
4000
6000
8000
10000
12000
14000
16000
18000
20000
Exposed side
Distance (microns)

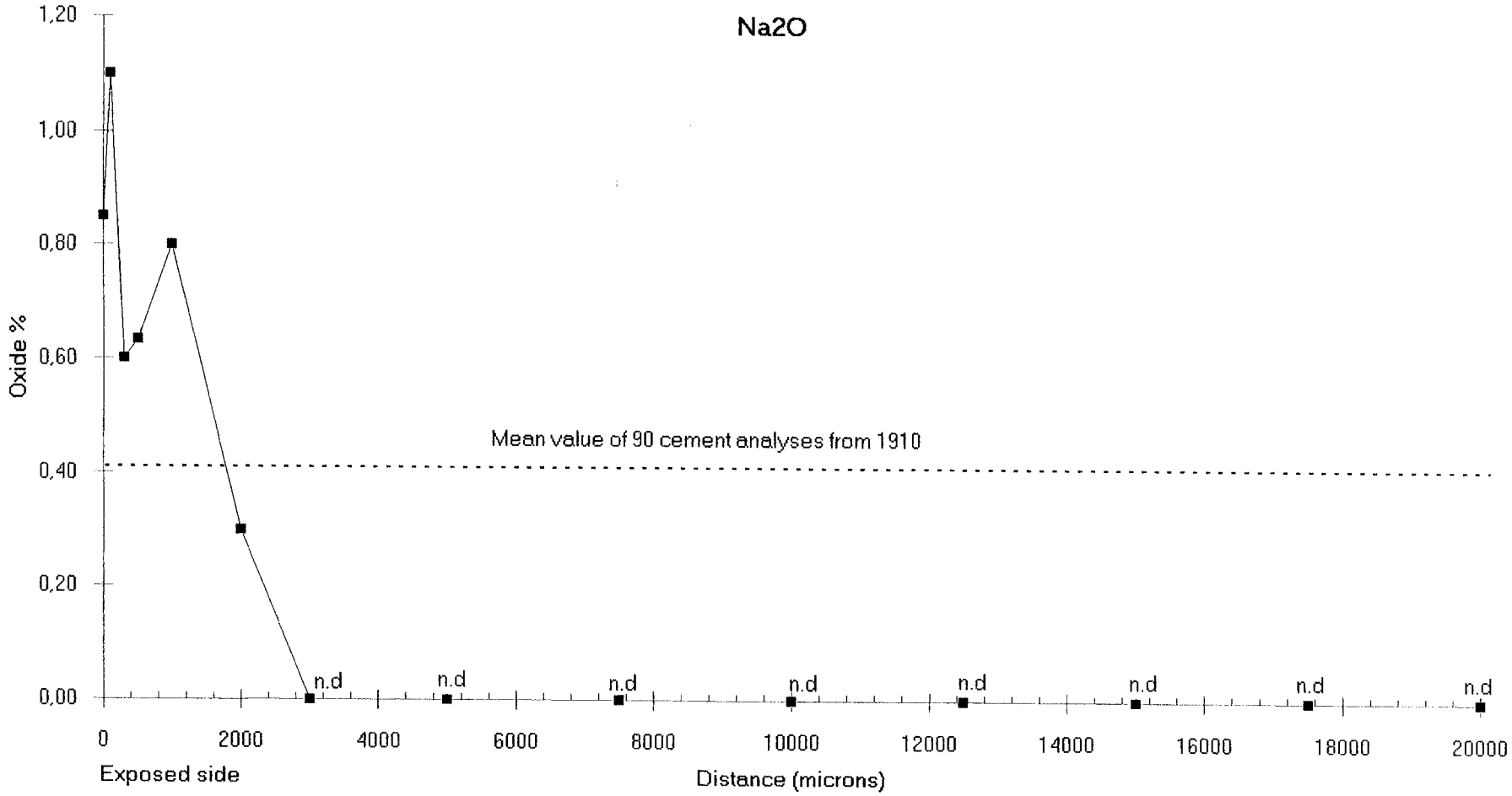
Na2O
1,20
1,00
0,80
0,60
0,40
0,20
0,00
Oxide %
Mean value of 90 cement analyses from 1910
n.d
n.d
n.d
n.d
n.d
n.d
n.d
n.d
0
2000
4000
6000
8000
10000
12000
14000
16000
18000
20000
Exposed side
Distance (microns)

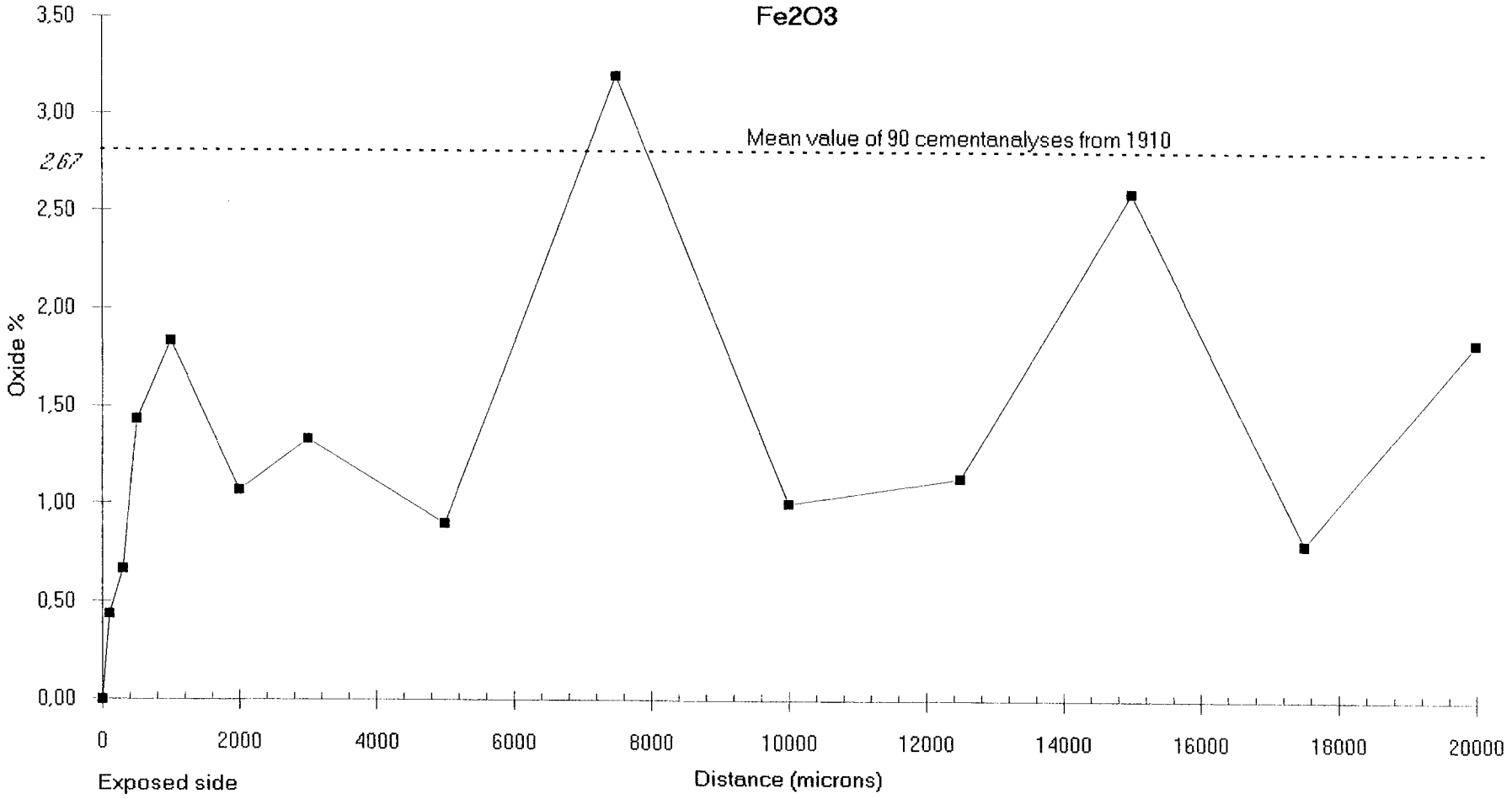
Fe2O3
3,50
3,00
2,67
2,50
2,00
1,50
1,00
0,50
0,00
Oxide %
Mean value of 90 cementanalyses from 1910
0
2000
4000
6000
8000
10000
12000
14000
16000
18000
20000
Exposed side
Distance (microns)

# *List of SKB reports*

## Annual Reports

*1977-78*
TR 121
**KBS Technical Reports 1 – 120**
Summaries
Stockholm, May 1979

*1979*
TR 79-28
**The KBS Annual Report 1979**
KBS Technical Reports 79-01 – 79-27
Summaries
Stockholm, March 1980

*1980*
TR 80-26
**The KBS Annual Report 1980**
KBS Technical Reports 80-01 – 80-25
Summaries
Stockholm, March 1981

*1981*
TR 81-17
**The KBS Annual Report 1981**
KBS Technical Reports 81-01 – 81-16
Summaries
Stockholm, April 1982

*1982*
TR 82-28
**The KBS Annual Report 1982**
KBS Technical Reports 82-01 – 82-27
Summaries
Stockholm, July 1983

*1983*
TR 83-77
**The KBS Annual Report 1983**
KBS Technical Reports 83-01 – 83-76
Summaries
Stockholm, June 1984

*1984*
TR 85-01
**Annual Research and Development Report 1984**
Including Summaries of Technical Reports Issued during 1984. (Technical Reports 84-01 – 84-19)
Stockholm, June 1985

*1985*
TR 85-20
**Annual Research and Development Report 1985**
Including Summaries of Technical Reports Issued during 1985. (Technical Reports 85-01 – 85-19)
Stockholm, May 1986

*1986*
TR 86-31
**SKB Annual Report 1986**
Including Summaries of Technical Reports Issued during 1986
Stockholm, May 1987

*1987*
TR 87-33
**SKB Annual Report 1987**
Including Summaries of Technical Reports Issued during 1987
Stockholm, May 1988

*1988*
TR 88-32
**SKB Annual Report 1988**
Including Summaries of Technical Reports Issued during 1988
Stockholm, May 1989

*1989*
TR 89-40
**SKB Annual Report 1989**
Including Summaries of Technical Reports Issued during 1989
Stockholm, May 1990

*1990*
TR 90-46
**SKB Annual Report 1990**
Including Summaries of Technical Reports Issued during 1990
Stockholm, May 1991

*1991*
TR 91-64
**SKB Annual Report 1991**
Including Summaries of Technical Reports Issued during 1991
Stockholm, April 1992

*1992*
TR 92-46
**SKB Annual Report 1992**
Including Summaries of Technical Reports Issued during 1992
Stockholm, May 1993

*1993*
TR 93-34
**SKB Annual Report 1993**
Including Summaries of Technical Reports Issued during 1993
Stockholm, May 1994

*1994*

TR 94-33

**SKB Annual Report 1994**

Including Summaries of Technical Reports Issued during 1994

Stockholm, May 1995

*1995*

TR 95-37

**SKB Annual Report 1995**

Including Summaries of Technical Reports Issued during 1995

Stockholm, May 1996

*1996*

TR 96-25

**SKB Annual Report 1996**

Including Summaries of Technical Reports Issued during 1996

Stockholm, May 1997

## List of SKB Technical Reports 1998

TR 98-01

**Global thermo-mechanical effects from a KBS-3 type repository. Summary report**

Eva Hakami, Stig-Olof Olofsson, Hossein Hakami, Jan Israelsson

Itasca Geomekanik AB, Stockholm, Sweden

April 1998

TR 98-02

**Parameters of importance to determine during geoscientific site investigation**

Johan Andersson[1], Karl-Erik Almén[2], Lars O Ericsson[3], Anders Fredriksson[4], Fred Karlsson[3], Roy Stanfors[5], Anders Ström[3]

[1] QuantiSci AB

[2] KEA GEO-Konsult AB

[3] SKB

[4] ADG Grundteknik KB

[5] Roy Stanfors Consulting AB

June 1998

TR 98-03

**Summary of hydrochemical conditions at Aberg, Beberg and Ceberg**

Marcus Laaksoharju, Iona Gurban, Christina Skårman

Intera KB

May 1998

TR 98-04

**Maqarin Natural Analogue Study: Phase III**

J A T Smellie (ed.)

Conterra AB

September 1998

TR 98-05

**The Very Deep Hole Concept – Geoscientific appraisal of conditions at great depth**

C Juhlin[1], T Wallroth[2], J Smellie[3], T Eliasson[4], C Ljunggren[5], B Leijon[3], J Beswick[6]

[1] Christopher Juhlin Consulting

[2] Bergab Consulting Geologists

[3] Conterra AB

[4] Geological Survey of Sweden

[5] Vattenfall Hydropower AB

[6] EDECO Petroleum Services Ltd.

June 1998

TR 98-06

**Indications of uranium transport around the reactor zone at Bagombe (Oklo)**

I Gurban[1], M Laaksoharju[1], E Ledoux[2], B Made[2], A L Salignac[2],

[1] Intera KB, Stockholm, Sweden

[2] Ecole des Mines, Paris, France

August 1998

TR 98-07

**PLAN 98 – Costs for management of the radioactive waste from nuclear power production**

Swedish Nuclear Fuel and Waste Management Co

June 1998

TR 98-08

**Design premises for canister for spent nuclear fuel**

Lars Werme

Svensk Kärnbränslehantering AB

September 1998

TR 98-09

**Test manufacturing of copper canisters with cast inserts Assessment report**

Claes-Göran Andersson

Svensk Kärnbränslehantering AB

Augusti 1998

TR 98-10

# Characterization and Evaluation of Sites for Deep Geological Disposal of Radioactive Waste in Fractured Rocks

Proceedings from The 3rd Äspö International Seminar, Oskarshamn, June 10–12, 1998-11-10

Svensk Kärnbränslehantering AB
September 1998